

Review

Seeing Colors: A Literature Review on Colorimetric Whole-Cell Biosensors

Georgio Nemer ^{1,2}, Mohamed Koubaa ^{1,*} , Laure El Chamy ³, Richard G. Maroun ²  and Nicolas Louka ² 

¹ Université de Technologie de Compiègne, ESCOM, TIMR (Integrated Transformations of Renewable Matter), Centre de Recherche Royallieu, CS 60319, CEDEX, 60203 Compiègne, France; georgio.nemer@utc.fr

² Laboratoire CTA, UR TVA, Centre d'Analyses et de Recherche, Faculté des Sciences, Université Saint-Joseph de Beyrouth, Beirut 1104 2020, Lebanon; richard.maroun@usj.edu.lb (R.G.M.); nicolas.louka@usj.edu.lb (N.L.)

³ Laboratory of Biodiversity and Functional Genomics, UR-EGP, Faculty of Science, Université Saint-Joseph de Beyrouth, Beirut 1104 2020, Lebanon; laure.chamy@usj.edu.lb

* Correspondence: m.koubaa@escom.fr

Abstract: Colorimetric whole-cell biosensors are natural or genetically engineered microorganisms utilized to detect target molecules and ions as indicators of pollutants and biological activity in the environment. Upon detection, within specific concentration ranges which vary depending on the microorganism and its genetic circuitry among other factors, these sensors produce pigments which can be detected with the human eye past certain thresholds and quantified using simple analytical techniques, namely spectrophotometry. These sensors, which can be rendered portable through lyophilization and other methods, provide valuable and reliable substitutes of more demanding analytical ex situ techniques. The insights gained from this review can highlight technological progress in the field and contribute to the identification of potential opportunities afforded by these advancements.

Keywords: whole-cell biosensors; pigments; quantification; qualification; spectrophotometry



Citation: Nemer, G.; Koubaa, M.; El Chamy, L.; Maroun, R.G.; Louka, N. Seeing Colors: A Literature Review on Colorimetric Whole-Cell Biosensors. *Fermentation* **2024**, *10*, 79. <https://doi.org/10.3390/fermentation10020079>

Academic Editor:
Mekala Venkatachalam

Received: 24 December 2023

Revised: 17 January 2024

Accepted: 19 January 2024

Published: 25 January 2024



Copyright: © 2024 by the authors. Licensee MDPI, Basel, Switzerland. This article is an open access article distributed under the terms and conditions of the Creative Commons Attribution (CC BY) license (<https://creativecommons.org/licenses/by/4.0/>).

1. Introduction

A biosensor is a measurement or quantification system relying on a biological component to recognize target analytes [1]. These devices quantify biological activity or chemical composition through the production of a dose-dependent signal [2]. Whole-cell biosensors (WCBs) are genetically engineered microorganisms capable of detecting and reporting a particular compound or analyte through the emission of a discernable signal using a stimulus-specific reporter system. WCBs are efficient and cost-effective means for obtaining in situ qualitative as well as quantitative information about the medium in which they are introduced. The precision of the readout is governed by a number of factors including the microbial chassis used as a sensor, its resistance to the concentration of the substance being quantified, and the metabolic burden incurred by the synthesis of the output molecule among others. While some biosensors are capable of producing a single readout in response to a specific analyte, others have been engineered to produce distinct concentration-specific outputs [3]. Broadly speaking, these systems utilize a sensing module which detects a specific target (e.g., ion, molecule, or metabolite) and transmits this stimulus to a reporting module which outputs a visible signal. A panoply of characterized biological sensing systems and signaling pathways could be implemented in WCB sensing mechanism design [4]. Transcriptional regulator systems integrate promoters responding to specific environmental constituents linked to engineered gene circuits [5], resulting in the expression or repression of the reporter genes when the promoter-specific compound or protein-ion complex is detected in the medium. Another system relies on a riboswitch comprising an RNA aptamer. Through a conformational change induced by specific metabolite or ligand-binding, the riboswitch may regulate the expression of reporter genes through different mechanisms:

halting reporter transcription through the inhibition of antiterminator or the cleavage of mRNA, or activating or repressing translation via the sequestration of the ribosomal binding site (RBS) [6,7]. In essence, WCBs exploit the sensitivity of natural regulatory systems crucial to the survival of microorganisms [8]. They can be utilized for multifarious purposes, such as monitoring natural environments like soil or bodies of water [9,10], screening for high-output strains in biosynthetic industrial settings [11], or providing health data by revealing the amounts of specific micronutrients in human serum among other uses [12].

While a number of microbial reporters can serve as output signals, microbial pigments offer considerable advantages in terms of convenience given that a simple visual examination or spectrophotometric analysis enables qualitative and quantitative evaluation, respectively [13]. Indeed, correlations between the amount of analyte detected by the sensor and the amount of pigment produced in response to this stimulus enable analyte quantification with relative ease within specific ranges specific to the sensor. The overall accessibility, specificity, and ease of use of colorimetric whole-cell biosensors have motivated the development of elaborate systems which allow increased sensitivity and combined detection of multiple analytes. This literature review seeks to comprehensively examine the state of scientific research regarding colorimetric WCBs as well as to present an updated list of the analytes which can be reliably quantified using these systems. It is thus hoped that bringing these advancements to the fore would contribute to the field by incentivizing work that draws on achieved success and strives to overcome existing limitations. A systematic analysis of scientific literature was undertaken to identify salient developments in this increasingly popular area of research, including the rationale behind the design of the genetic circuitry as well as the methodologies used to create them. Moreover, this review seeks to identify the compounds these colorimetric WCBs can now be used to detect in addition to the concentration ranges which can be reliably reported. The knowledge derived from this review can contribute to a more profound understanding of the technological advancements in the field, of the challenges yet to overcome, and of the possibilities which can be envisaged using these technologies.

2. Response of WCBs to Synthetic Molecules

Polychlorinated biphenyls (PCBs) designate a large category of synthetic organic molecules with high hydrophobicity. The potential health complications engendered by PCBs are multitudinous and include neurological conditions, endocrine disruptions, and cancer [14]. Before their worldwide ban through the Stockholm Convention on Persistent Organic Pollutants in 2001, which superseded their 1976 ban in the USA, PCBs were used in a broad range of applications including textiles, construction, transformer oils, and hydraulic equipment. Despite the interruption of their production, the noxious effects of PCBs persist given their capacity to cause complications at remarkably low concentrations. To that end, PCB sensors with sensitivities in the ppb domain had been devised [15,16].

The sensor developed by Gavlasova et al. harnesses the metabolic abilities of *Pseudomonas* sp. P2 [17]. This strain isolated from a PCB contaminated soil, can, in the presence of biphenyl, convert PCBs into chlorobenzoic acid following a four-step catabolic pathway (Figure 1) [18,19].

In its penultimate step, the pathway engenders the formation of readily observable yellow HOPDA. Through its maximum absorbance at $\lambda = 398$ nm, HOPDA produced by *Pseudomonas* sp. P2 can qualitatively signal the presence of PCBs and semi-quantitatively determine their amounts. While a protocol leveraging HOPDA synthesis had been previously devised by Kuncova et al. [20], suboptimal immobilization of the bacterial cells on glass beads resulted in inaccurate quantification. The innovative aspect of the protocol developed by Gavlasova and colleagues lies in its use of tetramethylorthosilicate (TMOS) to immobilize the homogeneously dispersed WCB on 3 cm petri dishes. In addition to producing more reliable results, the immobilization method drastically reduced the detection time from several days to a few hours. The method proved particularly effective in providing accurate estimates of the concentrations of 2,3,40-trichlorobiphenyl, 2,4,40-trichlorobiphenyl,

and 2,5,40-trichlorobiphenyl. The method could enable a broad screening of soil samples before higher precision quantification using the standard methods of gas chromatography or high-pressure liquid chromatography.

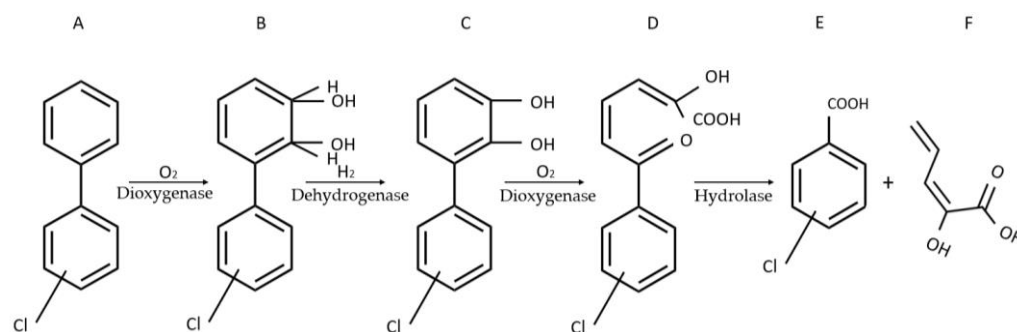


Figure 1. Four-step catabolic pathway of PCBs in *Pseudomonas* sp. P2. Adapted from Gavlasova et al. [17]. (A) biphenyl; (B) 2,3-dihydro-2,3-dihydroxybiphenyl; (C) 2,3-dihydroxybiphenyl; (D) 2-hydroxy-6-oxo-6-phenyl-2,4-hexadienoic acid (HOPDA); (E) benzoic acid; (F) 2-hydroxy-2,4-pentadienoic acid.

With its myriad chemical compositions and physical properties, soil nurtures numerous interdependent systems of flora and fauna influenced by its attributes and which, in turn, influence its composition. As such, deleterious alterations made to any component of this system can inevitably yield commensurate ripple effects with enduring consequences. Human agricultural activity has entailed the use of a number of pesticides with considerable impact on animals and human health [21]. A number of optical biosensors have been devised to detect organophosphate pesticides through their hydrolysis products, chief among which is 4-nitrophenol [22]. However, the usability of these biosensors is limited given their limited portability.

To detect the hydrolysis products of organophosphate pesticides, Chong and Ching successfully produced an *E. coli* colorimetric WCB using a modified DmpR transcriptional activator, which allowed greater effector specificity and thus higher expression level of its cognate promoter driving the expression of the monomeric red fluorescent protein 1 (*mRFP1*) reporter gene [13]. While lycopene would be an obvious choice should a red pigment be considered as the output signal, the researchers stipulate that the synthesis of lycopene and carotenoids in general is highly influenced by metabolic fluxes. These variabilities might result in inconsistent results from a color intensity perspective and an incubation time standpoint. The use of readily visible red fluorescent proteins, expressed through *mRFP1*, was deemed likely to engender more dependable results [13]. Transcription regulator DmpR, widely investigated in phenol detection contexts [23–25], was used as a sensing module in a wholly mutagenized form. To select 4-nitrophenol sensing mutants most conducive to discernable red fluorescent protein (RFP) synthesis, the researchers used DmpR as a sensing module and *mRFP1* as a reporter module. *DmpR* was mutagenized randomly before reconstituting the sensor plasmid and transforming it into *E. coli* MG1655. The transformed *E. coli* strains were cultured on LB agar plates and, after accounting for possible false positives, two 4-nitrophenol-effected *DmpR* mutants DM01 and DM12 with adequate pigment basal expression were retained. Each of the transcription regulators was cloned onto a plasmid bearing *oph*, a gene encoding organophosphorus hydrolase or OPH, and *mRFP1* to create novel sensor plasmids. Organophosphorus hydrolase enables the hydrolysis of parathion into 4-nitrophenol and thus its detection through DM01 and DM12, followed by the induced synthesis of RFPs. The novel biosensors were able to signal the presence of both hydrolyzed and unhydrolyzed organophosphorus pesticides. The synthesis of organophosphorus hydrolase (OPH) commensurably affected the effectiveness of the sensor and, to overcome this bottleneck, a strong constitutive promoter *pTet* was selected to drive the expression of the *oph* gene in the engineered DM01 and DM12 mutant *E. coli* strains. Moreover, to shift from cytoplasmic OPH secretion to a more efficacious

periplasmic secretion, the signal peptide of wild type OPH was replaced with the twin-arginine signal peptide of triethylamine N-oxide reductase. The effectiveness of these newly engineered strains was assessed and compared to the activity of an analogous control strain utilizing the regulatory mutant DmpR-E135K, which was reported to possess an enhanced response to 4-nitrophenol [24]. Compared to the latter which exhibited a detection threshold of 50 μ M for parathion, the detection threshold for the DM12 and DM01 strains was 10 μ M. DM12 and DM01 also had lower detection thresholds for fenitrothion of 100 μ M and 50 μ M, respectively, compared to the DmpR-E135K mutant, which produced more modest amounts of pigment at 100 μ M. Given that DM01 had greater basal RFP synthesis which could engender false positives, DM12 was deemed to be the better overall sensor for organophosphate detection, with RFP evincing the presence of these pesticides within 6 h of incubation. Having observed no significant improvements after switching to membrane defective *E. coli*, the researchers concluded that the transfer rate of 4-nitrophenol into the cytoplasm was not a limiting factor.

The ramifications resulting from soil contamination are substantial, even when the leaching of these contaminants into aquifers and bodies of water is not accounted for. Indeed, despite its ostensible abundance, topsoil is a relatively scarce resource naturally formed through a lengthy process resulting from the convergence of numerous factors such as precipitations, topography, local flora and fauna, as well as parent material [26]. In addition to its disproportionate degradation as a result of unsustainable agricultural practices, topsoil is naturally subjected to climate-dependent erosion [27]. As such, soil contamination exacerbates an ongoing problem threatening plant and animal life as well as the biological processes allowing for carbon sequestration and thus the mitigation of man-made climate change. Given the breadth and magnitude of consequences stemming from soil contamination, making accessible tools available to researchers and field technicians is a strategic imperative in the developed world and in developing countries alike. Colorimetric whole-cell biosensors are compatible with these exigencies and can enable the assessment of possible contaminations resulting in the development of apt bioremediation strategies.

3. Detection of Metals by WCBs

Heavy metals have been integrated in a broad array of anthropogenic activities and have agricultural, medical, or industrial applications among others. This ostensible ubiquity of heavy metals has greatly enhanced their odds of eventually wasting into ecosystems and engendering a number of health-related hazards for flora and fauna alike [28]. In addition to their bioaccumulation and dose-dependent toxicity to humans and animals, heavy metals affect soil fertility and thus plant yield [29]. Thus, it is of great importance to develop appropriate means for the detection and quantification of heavy metals.

3.1. Response of WCBs to Copper

Copper (Cu), among other metal ions such as zinc and manganese, plays a significant role as an enzyme cofactor involved in the catalysis of metabolic activity and the maintenance of cell integrity through osmotic pressure regulation [30]. Despite its considerable utility, copper becomes harmful to humans, animals, and plants alike past respective thresholds, and colorimetric WCBs can provide reasonable data regarding its concentration in water bodies. Several copper metalloregulator systems have been characterized in a number of microorganisms. In *Saccharomyces cerevisiae* for example, metallothionein encoded in *CUP1* enables the chelation of Cu(II) ions and protects the cell from copper poisoning. The copper-dependent DNA-binding protein ACE1 induces *CUP1* transcription through the binding of ACE1-Cu(II) complex onto the upstream activation sequence of *CUP1* [31].

A colorimetric WCB consisted of an engineered strain of *S. cerevisiae* with a deleted *ADE2* gene, encoding phosphoribosylaminoimidazole carboxylase, and a *CUP1* promoter *PCUP1* driving the expression of genes at the *ADE5,7* locus encoding glycineamide ribotide synthetase and aminoimidazole ribotide synthetase [32,33]. In this strain dubbed BY-*ade2-PCUP-ADE5,7*, the *CUP1* promoter, being inducible mainly by Cu(II) ions [34], leverages

the adenine monophosphate pathway altered by *ADE2* deletion to enable intracellular accumulation of red pigments in the yeast in high Cu(II) and high O₂ environments, resulting in visible color changes commensurate with Cu(II) concentration. The modified *S. cerevisiae* cells were immobilized in alginate beads and the accumulation of red pigment was found to accurately correlate with Cu(II) concentrations within the 1–100 µM range. The relatively simple biosensor provides a readout following an overnight incubation in the water to be tested.

A *Cupriavidus metallidurans* CH34-based biosensor was developed to quantify Cu(II) ions in aquatic environments through the expression of yellow betaxanthin pigments [35]. *C. metallidurans* possesses the copSR regulatory system, which grants the microorganism the ability to thrive in environments with high copper levels. To produce an effective biosensor, different promoters of the *cop* cluster identified in the organism's genome—*PcopT*, *PcopQ*, *PcopH*, *PcopA*, and *PcopM*—were first evaluated in red fluorescent protein biosynthesis assays. To identify the ideal promoter, plasmid backbones bearing *copS-copR* sequences under the control of native promoter and one of the candidate *cop* promoters driving the expression of reporter gene *rfp* were each transformed into *C. metallidurans*.

Having selected *copQ* as the promoter producing the results evincing the most reliable linearity between Cu(II) concentration and red fluorescent protein synthesis as well as the highest selectivity to Cu(II) (Figure 2), the researchers thus constructed the recombinant strain carrying a *PcopSR-copS-copR-PcopQ-Mjdod* construct. Reporter module *Mjdod*, encoding DOPA 4,5-dioxygenase, enabled the synthesis of visually discernable betaxanthin when substrate L-DOPA was available and the output from the colorimetric biosensor outmatched that of the fluorescence-based biosensor from a detection time perspective. This enabled the researchers to obtain dose-dependent colorimetric readouts in 6 h and within the 0–1000 µM range. Compared to its fluorescent counterpart, the colorimetric sensor produced a readout after a more modest incubation time.

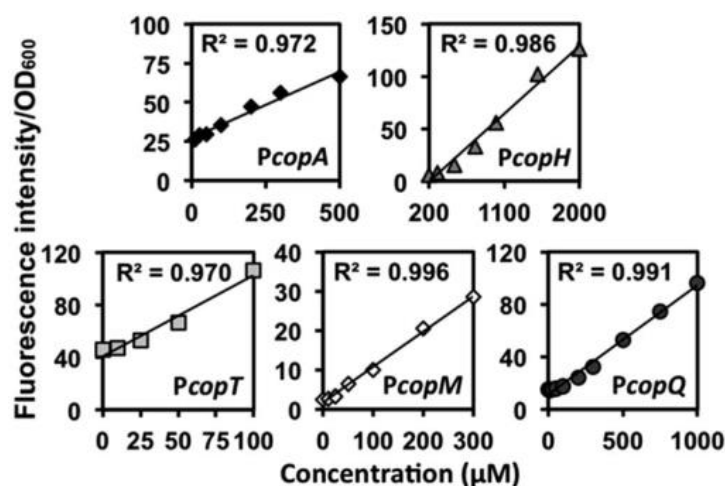


Figure 2. Results from the RFP assay evincing linearity between Cu(II) concentration and RFP output. Reproduced from [35] with permission from the Royal Society of Chemistry.

A number of in situ commercial copper testing kits can be utilized to test samples drawn from bodies of water or domestic water supply systems with sensitivities ranging from the ppm range to the mg range. Compared to these commercial tests, the described WCBs can be used in much wider concentration ranges and can provide results with higher exactitude.

3.2. Response of WCBs to Cadmium

Colorimetric WCBs can, in low-resource areas, supplant more complicated and voluminous equipment and enable in situ analyses. Cadmium (Cd) constitutes a source of considerable disruptions within ecosystems given its bioaccumulation, toxicity, and persis-

tence in the environment [36]. A host of WCBs have been devised to detect Cd among other heavy metals and include fluorescent, chemiluminescent, and bioluminescent reporters. A number of Cd-specific metalloregulators have been used in various biosensors to reveal the presence of Cd. Most saliently in the context of WCBs, *CadR*, which is categorized under the *MerR* subfamily of metal-ion-sensing transcriptional regulators with variable specificities and was characterized in *Pseudomonas aeruginosa* [37], regulates its own transcription as well as that of a Cd efflux P-type ATPase *CadA*, thus making microbial species resistant to high concentrations of the metal.

The Phytoene dehydrogenase (*CrtI*)-enabled synthesis of red carotenoid pigment deinoxanthin from colorless substrate in *Deinococcus radiodurans* was leveraged to produce a Cd-selective biosensor [10]. In this instance, *D. radiodurans* was engineered to exclusively produce deinoxanthin in the presence of Cd(II). To achieve this, the researchers utilized a colorless strain of *D. radiodurans* dubbed KDH018, whose *crtI* gene had been previously deleted, as the WCB chassis. To use red deinoxanthin as a reporter, and using *E. coli* for all genetic manipulations, *crtI* was cloned from chromosomal DNA of wild-type *D. radiodurans* onto a pRADZ3 *E. coli* to *D. radiodurans* shuttle vector, thus generating pRADI [38]. Four Cd-responsive genes *DR_0070*, *DR_0659*, *DR_0745*, and *DR_2626* in the *D. radiodurans* genome had been identified in an earlier work [39]. The Cd-inducible promoters of these genes were evaluated in the present study using a β -galactosidase activity assay to identify the one inducing greater reporter expression. To that end, each of them was cloned onto a pRADZ3 shuttle plasmid in such a way as to replace the putative *groESL* promoter driving *LacZ* expression, and *D. radiodurans* was used as the sensor chassis. The *DR_0659* promoter was selected. Operating on the principle that smaller promoters are more advantageous in the construction of expression cassettes with multiple reporter genes, the researchers attempted to remove promoter fragments to determine the minimal fragment required to equip *D. radiodurans* with a Cd-inducible response apparatus. The 393 bp fragment dubbed *P0659-1* was cloned onto pRADI to yield pRADI-P0659-1 which was subsequently transformed into KDH018. The resulting biosensor could reliably signal the presence of Cd(II) in the medium within the 50 nM–1 mM range and the concentration threshold beyond which the color can be detected by the human eye was 50 nM. Beyond the upper limit of the range, there was no noticeable deepening of the red color, and a diminution of intensity was noted above 200 mM.

While microorganisms with inherent Cd(II) resistance are conspicuous candidates to explore in this context, model organisms such as *E. coli* can also be utilized to this end. To detect Cd(II) ions in environmental water with relatively high specificity, a violacein-producing colorimetric biosensor was devised using *E. coli* as a chassis [40]. The sensory module consisted of the metalloregulator *cadR* gene, originally characterized in *Pseudomonas putida* [41], and its divergent *cad* promoter, whereas the reporter module consisted of a synthetic *vioABCDE* gene cluster, characterized in *Chromobacterium violaceum* [42], enabling violacein synthesis (Figure 3) [43].

The *CadR* gene had been used in earlier works detailing the development of fluorescent WCBs. Sensor plasmid pPcad-vio, which was developed in an earlier work and is discussed in greater detail in the upcoming section [43], bearing *CadR*, its divergent promoter, and the synthetic violacein cluster was transformed into *E. coli* TOP10, generating the TOP10/pPcad-vio engineered strain. Early exponential phase cultures of this strain were incubated in Cd(II) containing solutions for 3 h before the violacein concentration was evaluated following extraction using butanol as solvent. Hydrophobic violacein was quantified spectrophotometrically at $\lambda = 578$ nm. Cd(II) elicited a dose-specific response from the sensor up to 25 μ M (Figure 4) with the most substantial linearity occurring at the sub 2.5 μ M domain. Given the relatively poor albeit variable selectivity of *MerR* metalloregulators, a dose-specific response to the mercury ion Hg(II) up to 10 μ M was observed.

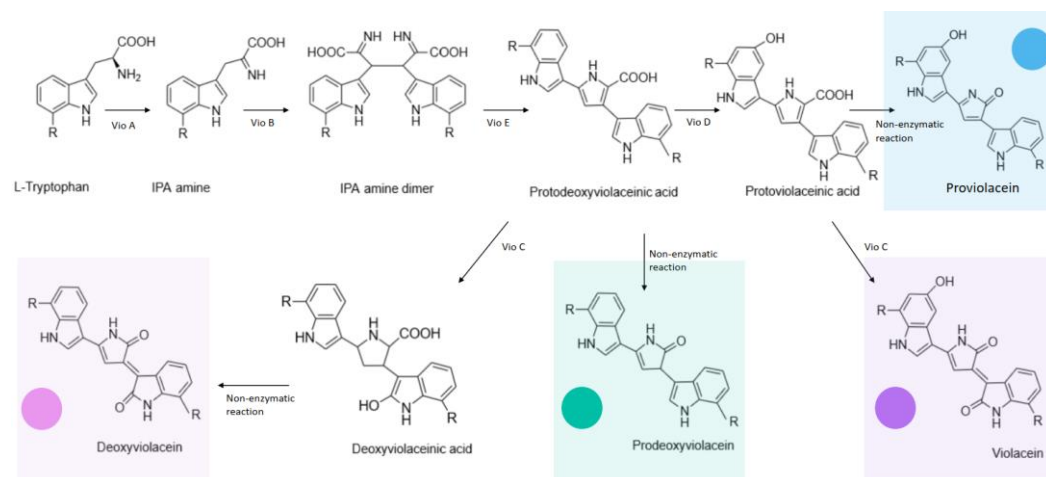


Figure 3. Enzymatic and non-enzymatic reactions implicated in the violacein biosynthetic pathway encoded by the *vioABCDE* cluster, as well as the different colored products they yield.

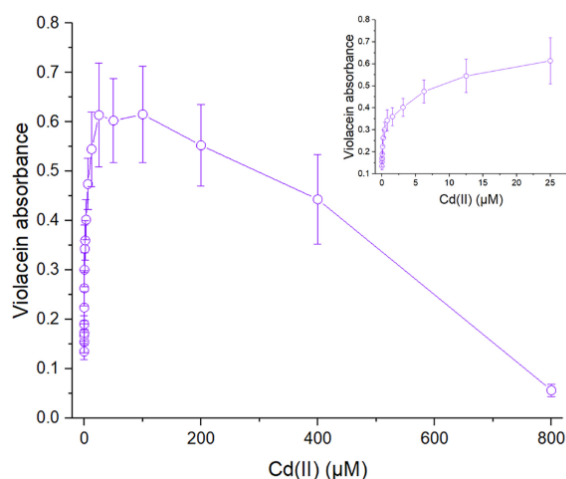


Figure 4. Violacein absorbance value as a function of Cu(II) concentration in the culture medium. ([40] with permission).

Despite this minor shortcoming, the sensor exhibited poor responsiveness to lead (Pb) and zinc (Zn). Indeed, metalloregulator proteins capable of sensing Cd(II) exhibit difficulties discriminating Cd(II) from Pb(II), Zn(II), and Hg(II) [44]. The fact that this generality holds true only to a modest degree in this instance is attributable to the fact that the *cad* promoter is most responsive to Cd(II) by a significant margin compared to other metal ions [45,46].

Another method of detecting Cd(II) using the *CadR* sensor module and *E. coli* TOP10 competent cells as a host used a previously assembled indigoidine biosynthesis module, comprising a *Streptomyces lavendulae* derived *bpsA* encoding a non-ribosomal peptidesynthase and a *pcpS* derived from *Pseudomonas aeruginosa* PAO1 encoding a 4'-phosphopantetheinyl transferase (PPTase) to activate apo-BpsA [47], as a visual reporter system and red fluorescent protein as a fluorescence-based reporter [9]. BpsA catalyzes the production of the readily detected blue pigment indigoidine with L-glutamine as a substrate. In an earlier work, the researchers detailed the development of a fluorescence-based Cd-detecting biosensor utilizing mCherry red fluorescent protein as a reporter [48]. This endeavor relies on the utilization of the pCadR-R genetic construct conceived in this earlier work which consists of a pET-21a derivative containing *CadR* and the divergent *cadR* promoter region as well as a promoterless *mcherry*. To construct the dual output sensor, the synthetic indigoidine biosynthesis module was cloned into a pET-21a plasmid, thus generating pT7lac-ind. The

Pseudomonas putida derived DNA fragment bearing the *CadR* gene and the divergent *cad* promoter, which had been previously cloned onto pCadR-R [48], were amplified along with *mcherry* from the pCadR-R plasmid using PCR and subcloned into the pT7lac-ind to generate pCad-ind-R which was transformed into *E. coli* TOP10. Lag phase cultures of the engineered strain exhibited a pronounced dose-dependent response to Cd(II) through their fluorescent and colorimetric reporters. Additionally, they exhibited modest responses to other inducers Hg(II), Pb(II), and Zn(II). The optimal incubation time required for correct quantification was 4 h, and Cd(II) was reliably quantifiable colorimetrically up to 200 μ M at $\lambda = 600$ nm.

The Environmental Protection Agency (EPA) and the Food and Drug Administration (FDA) have set the upper limit of acceptable Cd concentration in drinking water to be 5 μ g/L (<https://cdc.gov>, accessed on 22 November 2023), which is well within the dose-dependent detection range of the presented sensors. While Cd could be quantified using an expanding roster of analytical techniques [49–52], an inexpensive quantification using colorimetric WCBs is a reasonable alternative.

3.3. Response of WCBs to Lead

Environmental lead (Pb) is either naturally occurring or resulting from anthropogenic activity given its use in automotive batteries, telecommunications, construction, and its erstwhile use in pipes and paints among others. The toxicity threshold of lead to humans and animals is quite low, with chronic exposure resulting in anemia, neurotoxicity, and severe renal damage [53]. *PbrR*, a transcriptional regulator and part of the *MerR* subfamily, mediates the Pb(II)-induced transcription from its divergent promoter and regulates the *pbr* operon as part of some microorganisms' lead detoxification systems [54]. The *pbr* operon was first identified in *Cupriavidus metallidurans* CH34 and encodes a particularly comprehensive Pb resistance mechanism which entails transport, efflux, sequestration, precipitation, and biomineralization [55]. As such, components from the *pbr* operon can and have been successfully utilized in the conception of Pb-sensing WCBs producing various readouts [56–58].

The indigoidine reporter module described earlier was also utilized in conjunction with a Pb(II) sensory module comprised of the *PbrR* transcription regulator and its divergent promoter [47]. The DNA fragments bearing *pbrR* the *pbrR*-divergent *pbr* promoter, borne on the pT-Ppbr plasmid constructed in an earlier study [59], were amplified and cloned into the pT7lac-ind plasmid to yield pPpbr-ind, which was then transformed into *E. coli* TOP10 competent cells. The output signal is reliably produced 3 h post-incubation with the inducer present, and it can be spectrophotometrically assessed at $\lambda = 600$ nm to derive the concentration of bioavailable Pb(II). The authors noted that WCBs harvested at the lag phase were more apt at detecting Pb within the 0.13–4.17 μ M range, whereas those harvested at the exponential phase produced the best results within the 0.26–8.3 μ M range. While a color change detectable by the human eye can only be observed at 4.17 μ M, the method is still conducive to a rapid and reliable spectrophotometric assessment of Pb content in waters suspected of contamination.

Pb(II)-dependent metalloregulator protein *PbrR* was also used as a component of a sensory module in an *E. coli* TOP10-based WCB leveraging the violacein biosynthetic pathway [43]. The violacein synthetic pathway was first cloned onto a pET21a plasmid to yield pET-vio. Subsequently, the DNA fragment containing gene *pbrR* and its divergent promoter *Ppbr*, borne on the pT-Ppbr plasmid constructed in an earlier study [59], was PCR-amplified and cloned onto the pET-vio plasmid to yield pPpbr-vio used to transform *E. coli* TOP10. Three hours post-incubation in Pb(II)-containing media, the produced violacein could be extracted using butanol and quantified at $\lambda = 490$ nm. A linear relationship between Pb(II) concentration and violacein concentration was observed within the 0.1875–1.5 mM range. Beyond the upper limit of the range, the sensor exhibited qualitative properties up to 24 μ M, which was the highest tested concentration. An advantage proffered by the use of violacein in this sensor was the ability to visually detect amounts of Pb(II) in the medium at levels below 0.1875 mM.

Building upon this previously mentioned work, the researchers resorted to subcloning techniques to generate plasmids pPpbr-vioABE, pPpbr-vioABDE, and pPpbr-vioABCE from pPpbr-vio [60]. Each of the plasmids including pPpbr-vio was transformed into *E. coli* TOP10 to create four WCBs relying on different reporter pigments. The violacein- and deoxyviolacein-producing strains were retained for later assays given that the expected pigment output was produced as opposed to what was observed with the remaining strains. This occurrence can be attributed to the instability of prodeoxyviolacein and proviolacein intermediates as well as the highly branched metabolic pathway culminating in violacein synthesis [61]. The deoxyviolacein-based biosensor displayed considerable efficacy and a narrow dose-dependent response across a broad range of Pb(II) concentrations spanning 2.93–6000 nM, whereas the violacein-based one exhibited a less narrow dose-dependent response between 2.93 nM and 750 nM. Understandably, the researchers attributed to the considerably lessened sensitivity of the violacein-based biosensor to its comparatively high cytotoxicity and thus its deleterious effects on the heterologous host. Dependable readouts for both sensors can be obtained 3 h post-incubation, and violacein and deoxyviolacein can be quantified spectrophotometrically at $\lambda = 570$ nm and $\lambda = 579$ nm, respectively. Moreover, both sensors exhibited good selectivity for Pb(II) among other metal ions.

Sensory module *pbrR* continues to prove remarkably useful when used in conjunction with a bicistronic synthetic cyanidin 3-O-glucoside biosynthetic cassette (Figure 5), referred to as colored anthocyanidin derivatives or CACD in this study [62]. Genes from the biosynthetic cassette coding for 3-O-glycosyltransferase and anthocyanidin synthase were PCR amplified and cloned onto the previously referenced pPpbr-vio plasmid to generate pPb-CACD. The recombinant plasmid was transformed into *E. coli* TOP10 cells to create the *E. coli* TOP10/CACD biosensor.

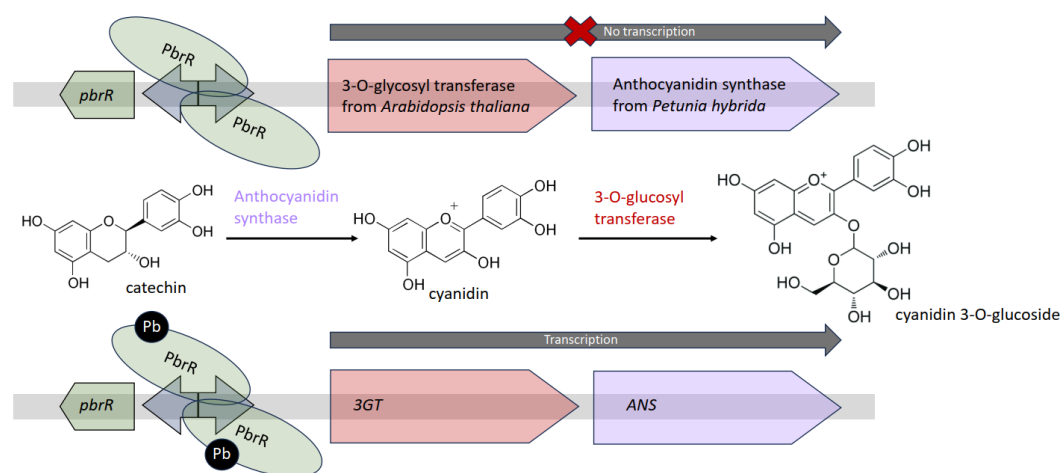


Figure 5. Pb-inducible expression of the cyanidin 3-O-glucoside biosynthetic pathway genes. Adapted from [62].

Upon detection of bioavailable Pb, the transcription of the reporter genes is initiated, and the synthesized enzymes act upon the substrate catechin to create CACD (Figure 5). The latter can be quantified at $\lambda = 428$ nm, although a number of publications reported that maximum absorption occurs at higher wavelength values [63,64]. A dose-dependent linear relationship between Pb(II) concentration and pigment absorbance value was observed within the 0.012–3.125 μ M range, although beyond this upper limit and up to 200 μ M, it functioned well as a qualitative sensor.

The EPA estimates that drinking water can account for 20% of a person's total exposure to Pb and sets the acceptability limit to 15 μ g/L, appropriately within the detection range of the sensors devised for this purpose. As such, lead sensing WCBs could be used to cheaply run routine tests without necessarily forgoing the need for precision analytical testing. Given their accessibility, they may also be used to run tests more frequently and

thus enable authorities to monitor water supply systems more thoroughly at an increased number of sampling points without a substantial increase in cost. Such recourse could help avert significant and far-reaching public health hazards such as the infamous 2014 Flint water crisis [65].

3.4. Response of WCBs to Mercury

The highly toxic nature of bioaccumulative mercury (Hg) coupled with its relative abundance in the environment make it a veritable hazard to public health. Several bacteria have developed resistance mechanisms to the metal. These detoxification mechanisms, enabled by an inducible set of genes arranged in a single *MerR* operon under the control of the metal-sensing MerR protein [66], have been exploited in a number of contexts to create crucial biosensors enabling the safeguarding of human and animal health.

The polyvalence of the indigoidine reporter module is further evinced in its robustness at signaling the presence of Hg(II) in an *E. coli*-based WCB [47]. This was achieved by coupling the reporter module with a sensor module consisting of the *MerR* gene encoding the metalloregulator protein MerR and its divergent *mer* promoter region, which had been synthetically produced and introduced into a pET-21a plasmid to generate Ppmer [67]. The DNA fragments contained in Ppmer were PCR amplified and cloned into the previously referenced pT7lac-ind plasmid to generate pPmer-ind, which was then transformed into *E. coli* TOP10. WCBs harvested at the exponential phase of bacterial development were found to reliably signal and quantify Hg(II), which induced a dose-responsive indigoidine biosynthesis at a concentration range spanning 0.008–0.52 μM , with the color of the pigment exceeding the human eye detection threshold at Hg(II) concentrations above 0.033 μM .

The violacein reporter developed by Hui et al. and utilized to detect Pb in an earlier work [43] was repurposed in the creation of a Hg(II) biosensor [68]. The Ppmer sensor module which was constructed by Zhang et al. [67] was also utilized in this undertaking. To assemble the sensory and reporter apparatuses, the researchers PCR amplified the DNA fragment containing *merR* gene and its divergent *mer* promoter from the Ppmer plasmid and cloned them into pET-vio to generate pPmer-vio. The recombinant plasmid was transformed into *E. coli* TOP10 to yield a Hg-sensing WCB which would respond to Hg by producing the violet pigment violacein. A dependable readout from WCB cells harvested during the exponential phase was obtained 5 h post-induction, and it exhibited a dose-dependent pigment-based response to Hg(II) in the range of 0.78–12.5 μM . Beyond this upper limit, violacein synthesis reportedly decreased as a result of toxicity. Inductive amounts of Hg(II) equal to and beyond 6.25 μM incurred the production of enough pigment to be detected by the human eye post-extraction using butanol. Sensors harvested at the lag phase exhibited a dose-dependent response to Hg(II) within the 0–0.12 μM range, thus allowing for the quantification of more minute amounts of Hg(II). Violacein was visible with the human eye post-extraction at Hg(II) concentrations withing the 0.006–0.098 μM range and the intensity of the violet color diminished past the Hg(II) concentration of 0.024 μM due to cytotoxic effects.

Transcription regulator MerR has also been used as a sensor module in a *P. aeruginosa* WCB employing reporter genes *phzM* and *phzS*, encoding for the enzymes methyltransferase and flavin-containing monooxygenase, respectively [69]. These enzymes catalyze the synthesis of pyomelanin [70], a red–brown pigment with potent antioxidative properties protecting microorganisms from oxidative stress [71]. A recombinant plasmid carrying *merR* under the control of native promoter and the *phzM* and *phzS* genes under the control of the *mer* promoter, was transformed into *P. aeruginosa* PAO1. The WCB worked well within a broad pH range, proved to be highly selective by responding poorly to other metal ions and produced a dose-dependent response to Hg(II) between 25 and 1000 nM. Prior to spectrophotometric quantification of pyocyanin to derive Hg(II) concentrations, the hydrophobic pigment must be extracted from the cells using chloroform and hydrochloric acid. Dissolved in the extraction solvent, the pigment exhibits a blue green color, enabling

pigment quantification at $\lambda = 520$ nm and consequently a reliable quantification of Hg(II) within the 25–1000 nm range.

To detect inorganic mercury in water samples, Hui et al. developed an *E. coli* Rosetta (DE3) based biosensor using β -carotene as a reporter [37]. The rationale underpinning the decision to rely on β -carotene rather than lycopene is that lycopene's potency as an antioxidant could result in rapid depletion and consequently a disappearance of the red color. Using *E. coli* TOP10 as a gene cloning host, the researchers cloned an *E. coli* codon optimized lycopene synthetic gene cluster comprising the genes *crtE* (encoding geranylgeranyl phosphate synthase), *crtB* (phytoene synthase), and *crtI* (phytoene desaturase) onto a pET-21a vector plasmid to produce pET-crtEBI. Subsequently, gene *crtY* enabling the conversion of lycopene to β -carotene was fused to the recombinant gene cassette to yield pET-crtEBIY. The sensing module consisting of an artificial *mer* operon-*merR* gene and its *mer* promoter [67], was cloned into pET-crtEBIY to yield pPmer-crtEBIY (Figure 6).

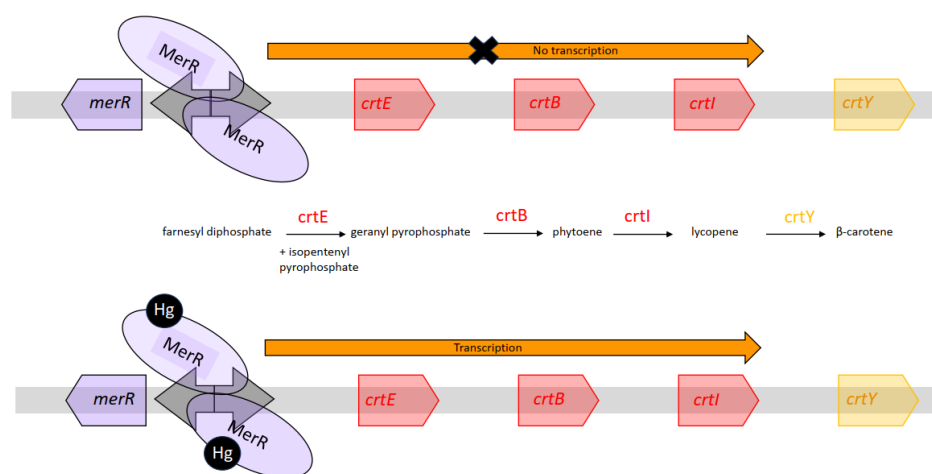


Figure 6. Inorganic Hg-dependent transcription of the genes involved in the β -carotene synthesis pathway. Adapted from [37].

To enhance the transcription of the genes involved in the β -carotene synthetic pathway and the expression level of *CrtEBIY*, an independent *mer* promoter was introduced upstream of each of the cloned genes. The plasmid was transformed into *E. coli* Rosetta, and assessments regarding selectivity and sensitivity were undertaken. The artificial *mer* operon was devised to mitigate selectivity issues inherent to MerR metalloregulators whereby metalloregulators specific to a metal would induce transcriptional activity when exposed to other metals. In this instance, response to non-mercury metals was negligible compared to that induced by Hg(II). A dose dependent response was observed within 3 h of incubation between 12 to 195 nM. The pigments could be quantified spectrophotometrically at 452 nm following an ethanol extraction.

3.5. Response of WCBs to Arsenic

Over one hundred million people are effected by arsenic (As) water contamination across the world and are thus prone to developing skin lesions and gastrointestinal distress in case of chronic exposure to low doses, although high concentrations pose a much greater toxicity risk to human health [72]. A number of WCBs were elaborated utilizing the *ars* operon, which consists of two regulatory genes (*arsR* and *arsD*) and three structural genes (*arsA*, *arsB*, and *arsC*) and contributes to arsenite and arsenate resistance by detoxifying the cell [73]. Highly contaminated areas include Indian and Bangladeshi industrial zones, and remediation must be enabled by access to cheap and dependable technologies.

The bright colors of carotenoid pigments spheroiden and spheroidenone were exploited in the creation of an arsenite biosensor [74]. In its wild form, photosynthetic bacterium *Rhodovulum sulfidophilum* produces the red pigment spheroidenone in semi-

aerobic conditions via the spheroidone pathway enabled by genes *crtF* and *crtA*. The former encodes for O-methyltransferase which acts upon the C-1 hydroxy group of demethyl-spheroidene resulting in the synthesis of yellow spheroiden, and the latter codes for a monooxygenase subjecting the spheroiden produced in the earlier step to a C-2 ketolation thus yielding red spheroidenone. As such, a mutant strain with the *crtA* gene deleted, such as *R. sulfidophilum* CDM2, would accumulate yellow pigments. To create the arsenite sensor, Fujimoto et al. relied on a strategy predicated on a color shift from yellow to red using *R. sulfidophilum* CDM2. To that end, they constructed a reporter module consisting of a promoter-less fragment of the *crtA* gene which was cloned onto a broad-host-range plasmid pRK415 together with the *E. coli*-derived sensory module comprising the arsenite responsive *E. coli* DNA fragment containing the operator/promoter of the *ars* operon (*O/pars*) as well as the *arsR* repressor. The recombinant plasmid, pSENSE-As, was transformed into *E. coli* S17-1 and transferred into *R. sulfidophilum* CDM2 through conjugation. Preliminary assessments confirmed that *E. coli* *O/Pars* was recognizable by CDM2 RNA polymerase and that no transcription repression by an endogenous protein occurred in CDM2. While the concentration threshold beyond which the sensor rendered arsenite presence observable with the human eye was 5 µg/L, the data proffered by the authors suggest that arsenite elicits a dose-dependent response in the sensor whereby the percentage of red pigment increases as the arsenite concentration does within the 2–8 µg/L range. However, the composition of the pigment load was assessed using HPLC, thus making the technique more qualitative than quantitative when utilized *in situ*. Moreover, the authors noted that the incubation time required for visual detection was at least 12 h, which could be a limitation if used in an off-site context.

A comparable endeavor was undertaken by Yoshida et al. using the lycopene-producing bacterium *Rhodopseudomonas palustris* [75]. During the synthesis of lycopene in *R. palustris*, phytoene dehydrogenase converts colorless phytoene into red lycopene. As such, the gene coding for phytoene dehydrogenase, *CrtI*, was selected as a reporter gene for the WCB whereby the detection of the target molecule would actuate a color shift from blue, the color of *CrtI*-deleted mutant strain *R. palustris* no. 711 [76], to red due to lycopene production. The expression of this reporter was placed under the control of a sensor module derived from the previously referenced pSENSE-As vector in pMG103 [74], an *E. coli*—*R. palustris* shuttle vector, to yield pMG103ΩParsarsRcrtIcat. The recombinant plasmid was then transferred into *R. palustris* no. 711 using electroporation. The resulting WCB reportedly exhibited a dose-dependent response to arsenite within the 1–10 µg/L range, with the color being easily distinguishable with the human eye at and beyond the 10 µg/L mark. The biosensor also exhibited good selectivity, responding poorly to antimony, arsenate, and Fe(II).

Heavy metal ions of natural or anthropogenic origins pose a serious and enduring threat to living organisms in the vicinity of contaminated sites [77]. Moreover, they can engender ripple effects in remote biomes and ecosystems which can be partly attributed to natural displacement phenomena. These effects are exacerbated by the migratory behavior of some affected species, which can be subject to scavenging or predation [78]. As such, the magnitude of the threat is substantial and duly warrants vast efforts with the aim of minimizing its impact [79–81]. To enable extensive and efficacious impact minimization endeavors, reliable and accessible detection technologies must be utilized across large areas to screen for heavy metals and concurrently undertake analyses. Such measures, be they reactive or proactive, can limit the rapidly spreading detrimental effects of abnormal heavy metal concentrations. Colorimetric WCBs are resource-efficient, and their accessibility makes them highly compatible with the scale of heavy metal pollution detection efforts and thus the volume of samples to be screened.

4. Biomonitoring and Control

4.1. High-Level Producer Detection

Lysine is an amino acid with considerable importance in the context of human and animal nutrition and is the second most abundantly produced essential nutrient worldwide [82,83]. *Corynebacterium glutamicum* is an effective production platform of L-lysine and other amino acids, and engineered strains have been turned into industrial workhorses specially created for this purpose [84]. Recent advances in the field have led to the development of the pSenLys biosensor based on the transcriptional regulator *LysG* which, in *C. glutamicum*, acts as a transcriptional regulator for *LysE*, the gene encoding amino acid exporter LysE, and detects variations in the concentrations of L-lysine, L-arginine, and L-histidine [85]. Various sensors have been developed using the pSenLys sensing module for the purpose of identifying overproducers, and a significant proportion of them relied on fluorescent reporters.

A notable drawback on pSenLys-based sensors is their inability to accurately report the overproduction of a specific amino acid among lysine, histidine, and arginine. The non-specificity of pSenLys prompted the exploration of different avenues. Liu et al. detailed the development of a *C. glutamicum* based colorimetric WCB with greater lysine specificity, utilizing lycopene as a reporter pigment [11]. In response to L-Lys, *LysG* activates the expression of *crtI* encoding phytoene desaturase which then catalyzes the production of lycopene with the characteristic red color. To that end, a *C. glutamicum* mutant strain, deficient of the carotenogenic gene cluster *crtIYefEb*, *crtB2I21/2*, and *LysEG* was first generated as a sensor chassis. To construct the plasmid, transcriptional regulator *lysG*; its binding site region *lysE* promoter; and the phytoene desaturase gene *crtI* were amplified using the genome of *C. glutamicum* as a template. The expression cassette was fused using overlap extension PCR and cloned into a pTRCmob vector plasmid dubbed pSensorI. The sensor plasmid was transformed into *C. glutamicum* WT- Δ *lysEG* Δ *crtIYebB22* and this transformed strain bearing pSensorI served as a control as other optimizations were implemented. To remedy the poor specificity of *lysG* and diminish false positives induced by docking of L-histidine and L-arginine, *LysG* was subjected to site-directed saturation mutagenesis to screen for mutants with reduced affinity to L-histidine and L-arginine. Substitutions at positions 123 and 125—where L-glutamate was substituted with L-L-tyrosine and where L-glutamate was replaced with L-alanine, respectively—were found to confer the modified binding site *lysG** a drastically reduced affinity to L-arginine and L-histidine and an uncompromised colorimetric linear response to L-lysine. To increase the range of dose-responsiveness up from the reported 40 mM limit, the researchers resorted to promoter engineering of *pLysE* and 5 promoters were screened. Promoter *pLysE-3* was selected as the most apt candidate and was found to engender an increased range of responsiveness of up to 300 mM. To enhance the performance of the sensor from a color-rendering standpoint and thus facilitate overproducer detection, the *CrtR* transcriptional regulator, which is known to repress the *crt* operon [86], was deleted by electroporating a suicide plasmid into WT- Δ *lysEG* Δ *crtIYebB2* to construct WT- Δ *lysEG* Δ *crtIYebB2R*. Further improving this performance was achieved by attenuating the impact of the rate-limiting step in carotenoid synthesis through an overexpression of phytoene synthase encoded by *crtB*. As such, the *crtB* gene cassette was added to the sensor plasmid to create pSenlysBI-3. Lycopene concentrations correlated very well with L-lysine concentrations, especially within the 80–325 mM range.

Comparable yield-increasing strategies would confer a considerable competitive advantage to manufacturers through targeted enhancements in production. Additionally, these manufacturers would be able to provide purer products to consumers who can derive greater benefit from them. From an environmental perspective, the amount of energy per gram of product would be reduced and these enhancements could result in fewer production cycles. As such, parts which can be energy-intensive to machine and ship would be replaced less often, further reducing the overall environmental toll of production.

4.2. Pathogen Detection

N-acyl homoserine lactone (AHL) is a signal molecule utilized by a number of gram-negative bacteria for cell-to-cell communication as part of the quorum sensing mechanism. The utility of WCBs leveraging the quorum sensing apparatus of microorganisms has a number of benefits namely signaling the presence of possibly pathogenic species [87], monitoring bacterial populations in bioreactor settings [88], and modulating the microbial composition of a medium [89].

N-butyryl-L-homoserine lactone (BHL) is an AHL and a small diffusible signaling molecule implicated in quorum sensing, the control of gene expression, and cellular metabolism [90]. To detect minute amounts of BHL within a wide concentration ambit, Yong and Zhong developed a *P. aeruginosa*-based biosensor [91]. The researchers used strain *P. aeruginosa* CGMCC 1.860, which is naturally capable of producing blue–green pigments upon detecting BHL. This is achieved through the RhlR-RhlI quorum-sensing system, which comprises the transcription activator protein RhlR and the BHL synthase RhlI [92]. To create a biosensor, the researchers deleted the *rhlIR* gene cluster, thus creating *P. aeruginosa* Δ rhlIR, and overexpressed *rhlR* through multi-copy plasmids. As such, the bacteria regained the capacity of sensing BHL while avoiding the production of the analyte by endogenous activity. The recombinant biosensor strain is thus capable of producing the pigment upon sensing of exogenous BHL which can diffuse in the cell and be recognized by the RhlR regulator. Upon BHL binding, this transcription regulator activates the expression of pigment synthases. The resulting WCB whose pigment output can be extracted using chloroform and quantified at $\lambda = 299$ nm exhibited dose-dependent pigment production within the 0.11–49.7 μ M AHL range.

To detect AHLs specific to *P. aeruginosa* and *Burkholderia pseudomallei*, two waterborne bacterial strains resistant to disinfection and environmental stress, Wu et al. developed a lycopene-producing biosensor [93]. To detect N-3-hydroxydecanoyl homoserine lactone, N-3-oxododecanoyl homoserine lactone, and N-decanoyl-L-homoserine lactone produced by *B. pseudomallei* and *P. aeruginosa*, the QscR quorum-sensing system was used as a sensing module in *E. coli*. In preliminary stages, the researchers used green fluorescent protein as a reporter. The sensing module consisted of the transcription factor QscR, placed under the control of a constitutive T7 promoter in plasmid pET23b(+), capable of binding to AHLs secreted by both bacterial strains. Upon its formation, the QscR-AHL complex binds to its proprietary binding site a QscR-AHL inducible promoter PA1897 thus engenders the activation of the reporting module EGFP, all components having been cloned into the pUC57kan plasmid. The sensor was found to respond well and selectively to the AHLs being investigated, and the detection threshold was found to be compatible with ecologically relevant amounts of AHLs. To produce the lycopene-based sensor, the lycopene production pathway was introduced in the biosensor by expressing genes *crtE* and *crtB* under the T7 constitutive promoter and expressing the gene *crtI* under the control of the PA1897 promoter in plasmid pET23b-qscR-EIB (Figure 7).

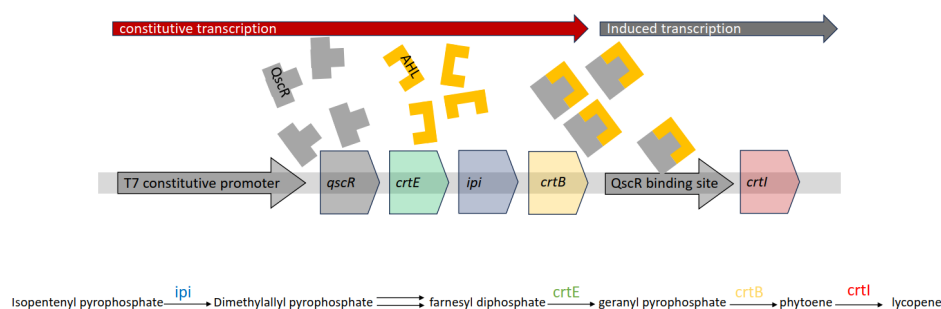


Figure 7. Functioning of the AHL-detecting colorimetric biosensor devised by Wu et al. [93].

To overcome a possible pigment production bottleneck, the *ipi* gene encoding the synthesis of isopentenyl pyrophosphate isomerase was introduced to convert available

isopentenyl pyrophosphate into dimethylallyl pyrophosphate. These constructs were cloned onto the pET23b-qscR plasmid to yield pET23b-qscr-EIB. The resulting biosensor was able to detect all three investigated synthetic AHLs at concentrations as low as 2.0×10^{-9} M, although the pigments synthesized in culture media wherein the target bacterial species had been cultured were less considerable in their amounts. This was attributed to a possible presence of molecules with an inhibitory effect on lycopene production.

The need to develop novel and rapid pathogen detection technologies is most pressing in our modern society with the disquieting rise of antibiotic resistant bacterial strains and their alarming spread [94]. Studies addressing bacterial antibiotic resistance have unearthed evidence that specific AHLs play a crucial role in the expression of drug resistance genes [95–98]. Consequently, fittingly engineered colorimetric WCBs immobilized on paper, for example, could provide highly useful information to healthcare professionals at points of care, triggering specific protocols. AHLs can be challenging to quantify given the fact that they can be subject to enzymatic degradation in the period between sampling and testing [99]. While this can be remedied with flash freezing using liquid nitrogen before subsequent analysis using a number of analytical techniques [99–101], quantification using WCBs can be an enticing alternative. Nevertheless, the inhibitory effects of unknown compounds resulting from bacterial proliferation and metabolic activity cannot be understated. As such, WCBs may be used in parallel with other analytical techniques to verify results.

4.3. Micronutrient Quantification

Micronutrient deficiencies are significant concern of global ambit although gauging the veritable magnitude of the issue remains challenging [102]. In remote settings and in impoverished parts of the world, access to reliable testing is limited due to elevated costs and logistical difficulties. Colorimetric WCBs as part of field-ready kits can be handled by agents with minimal training to provide in situ testing in remote areas, identify micronutrient deficiencies, and help remedy health complications quickly and reliably.

Zinc is an essential micronutrient; deficiencies have incurred public health burdens of significant magnitude, and one billion people across the world are presumed to be at risk of zinc deficiency [103]. Efforts to provide access to impoverished and remote areas of the world have yielded the development of colorimetric biosensors.

In the context of early efforts to develop a colorimetric biosensor compatible with zinc serum levels, Watstein and Styczynski generated an *E. coli*-DH10B-based sensor capable of producing three different reporters: violacein, lycopene, and β -carotene [12]. A violacein operon was cloned onto a plasmid bearing zinc-responsive transcription regulator *ZntR*, proprietary ribosomal binding sites, and the gene encoding the Zur metalloregulator protein, which acts as a zinc-responsive repressor. Gene cluster *viaABCDE* was placed under the control of a *PznuC* repressor actuated by Zur–zinc complexes. To modulate violacein production and ensure a violacein-dominated color profile within the 1–5 μ M zinc range and thus to counter increasing amounts of Zur–zinc complexes as zinc concentration increases, *zur* was placed under the control of the *ZntR* cognate promoter *PzntA* with an intermediate strength ribosomal binding site and 32 zinc decoy binding sites implemented. On another plasmid, the lycopene synthetic pathway was cloned from *Pantonea ananatis* and placed under the control of *PzntA* whereas *crtY*, the gene coding for lycopene β -cyclase, was placed under the control of *PznuC*. To ensure a lycopene dominated domain wherein zinc concentrations vary from just above 5 μ M to just under 20 μ M, a stronger ribosomal binding site to *PzntA* coupled with a LAA degradation tag were implemented to limit lycopene β -cyclase synthesis to the 20–100 μ M zinc concentration range.

To create a colorimetric WCB responding to physiologically relevant amounts of zinc in human serum, McNerney et al. devised a sensor with an observable pigment output which had been tuned to present a discernable dose-dependent optical readout [104]. The effort constitutes a continuation to the one described earlier. The system exploits several transcription activators, repressors, and reporters that allow to discriminately report alarming and healthy amounts of zinc in human serum. Should amounts of zinc

be alarmingly below the normal range, violacein would be the dominant pigment in the overall pigment load produced by the lyophilized cells resuspended in human serum. Should the amounts be cause for concern, the output would present as red due to lycopene being the prevailing component of the pigment matrix. Should the WCB be exposed to healthy amounts of zinc, the output would veer towards a yellow presentation given the prevalence of β -carotene in the pigment matrix. In this complex WCB system, the violacein synthesis gene cluster was placed under the control of an engineered *PLacZnu 2B* dual-input promoter created via the insertion of a mutagenized *zur* operator site downstream from the *Lac* promoter. This dual promoter allows the induced expression of the violacein gene cluster only at very low zinc concentrations. That same plasmid featured a zinc binding site *ZntR*, a *zur* gene with modified ribosomal binding sites, and an *ssrA* degradation tag to ensure optimal expression in such a method of rendering violacein synthesis taper down by 0.1 μ M zinc. On another plasmid, the researchers cloned the lycopene biosynthetic cluster *crtEBI* and a *crtY* lycopene β -cyclase gene with modified ribosomal binding sites and *ssrA* protein degradation tags. The former was placed under the control of a *Lac* promoter, whereas the latter was placed under the control of *PzntA* to ensure a dominant β -carotene-enabled orange presentation of the WCB at normal serum zinc levels and a red presenting lycopene-dominant presentation, evincing subpar zinc concentrations.

The colorimetric WCBs detailed in this section showcase their current usability in the healthcare sector as well as their ability to substitute, in varying degrees, conventional analytical techniques. WCBs have been developed to detect urinary tract infections [105,106] and inflammatory bowel disease [107,108], among other ailments as alternatives, to existing modalities with non-negligible drawbacks. The effectiveness of the sensor module—reporter module combinations that enable the aforementioned sensors may not be comparable to that of an analogous configuration featuring a colorimetric reporter module. However, should they prove effective, these colorimetric biosensors—among others—may enable on-site testing in use cases where such sensors are compatible. Table 1 summarizes the sensor module—reporter module combinations mentioned in this review as well as the analyte concentration ranges where they are most effective.

Table 1. Sensor module—reporter module combinations and their responsiveness.

Application	Sensory Module	Reporter Module	Pigment	Target Molecule	Range of Detection	Ref.
Quantification of PCBs	Biphenyl degradation pathway (unspecified genes)		2-hydroxy-6-oxo-6-phenyl-2,4-hexadienoic acid	Trichlorobiphenyl mixtures	0.5 mg D103 1-1 and 0.2 mg 2,4,40CB 1-1	[17]
Detection and quantification of organophosphate pesticides.	<i>DmpR—DM12</i>	<i>mRFP1</i>	RFP	parathion	10 μ M	[13]
	<i>DmpR—E135K</i>	<i>mRFP1</i>	RFP	fenitrothion	50 μ M	[13]
Detection and quantification of heavy metal ions in water	<i>PCUP1</i>	AMP pathway Δ ADE2	Unspecified red pigment	Cu(II)	1–100 μ M	[32]
	<i>PcopQ</i>	<i>Mjdod</i>	Betaxanthin	Cu(II)	0–1000 μ M	[35]
	<i>P0659-1</i>	<i>crtI</i>	Deinoxanthin	Cd(II)	50 nM–1 mM	[10]
	<i>cadR</i>	<i>vioABCDE</i>	Violacein	Cd(II)	0–25 μ M	[40]
	<i>cadR</i>	<i>bpsA, pcps</i>	Indigoidine	Cd(II)	0–200 μ M	[9]
	<i>PbrR</i>	<i>bpsA, pcps</i>	Indigoidine	Pb(II)	0.26–8.3 μ M	[47]
	<i>PbrR</i>	<i>vioABCDE</i>	Violacein	Pb(II)	0.1875–1.5 mM	[43]
	<i>PbrR</i>	<i>vioABCE</i>	Deoxyviolacein	Pb(II)	2.93–750 nM	[60]
	<i>PbrR</i>	<i>3GT, ANS</i>	Cyanidin 3-O-glucoside	Pb(II)	0.012–3.125 μ M	[62]
	<i>MerR</i>	<i>bpsA, pcps</i>	indigoidine	Hg(II)	0.008 μ M–0.52 μ M	[47]
	<i>MerR</i>	<i>vioABCDE</i>	Violacein	Hg(II)	0–0.12 μ M	[68]
	<i>MerR</i>	<i>phzM and phzS</i>	Pyomelanin	Hg(II)	25 and 1000 nM	[70]
	<i>MerR</i>	<i>crtEBI and crtY</i>	β -carotene	Hg(II)	12 to 195 nM	[37]
	<i>OPars</i>	<i>crtF and crtA</i>	Spheroiden and spheroidenone	Arsenite	2–8 μ g/L	[74]
	<i>OPars</i>	<i>CrtI</i>	Lycopene	Arsenite	1–10 μ g/L	[75]

Table 1. Cont.

Application	Sensory Module	Reporter Module	Pigment	Target Molecule	Range of Detection	Ref.
Identification of overproducers	<i>lysG</i>	<i>crtEBI</i>	Lycopene	Lysine	80–325 mM	[11]
Detection of bacterial contamination	<i>RhlI</i>	Blue-green pigment synthesis pathway native to <i>P. aeruginosa</i>	Unspecified blue-green pigment	N-acyl homoserine lactone	0.11–49.7 μ M	[91]
	<i>QscR</i>	<i>crtEBI</i>	lycopene	N-3-hydroxydecanoyl homoserine lactone, N-3-oxododecanoyl homoserine lactone, N-decanoyl-L-homoserine lactone	≥ 2.0 nM	[93]
Quantification of serum zinc	<i>Zur</i>	<i>VioABCDE, crtEBI, crtY</i>	Violacein, lycopene, β -carotene	Zn(II)	Physiologically relevant range	[12]
	<i>Zur</i>	<i>VioABCDE, crtEBI, crtY</i>	Violacein, lycopene, β -carotene	Zn(II)	Physiologically relevant range	[104]

5. Conclusions and Future Directions

The development of whole-cell biosensors keeps up with the pace of broad ranging advancements in genetic engineering and practically puts to use novel approaches stemming from recent advancements. As such, it allows for more nuance to materialize and for a greater understanding of processes and mechanisms to be gleaned. WCBs are a highly versatile platform enabling the development of accessible and inexpensive analytical devices which, in some circumstances, replace their less portable laboratory analogues [109]. They can be adapted to a considerable range of analytes that grows as more regulatory as well as biosynthetic pathways are characterized. Moreover, they benefit from a wide selection of thoroughly understood microbial chassis to transform based on the biosensor's purpose. The works detailed in this review attest to the effectiveness of colorimetric WCBs but also detail some of their less conspicuous shortcomings. Indeed, the caveat of these assessments being conducted in highly controlled settings must be borne in mind. In effect, they were mostly undertaken using solutions of known analyte concentrations and compositions. Their effectiveness in the field may be less pronounced due to a host of causes including the general complexity of natural matrices which may contain compounds of bacterial origin or otherwise which may affect their performance or result in false positives and negatives. Moreover, living organisms have a limited shelf life, and stocks will require periodic replenishment. Despite these shortcomings, WCBs can be an advantage for researchers in settings presenting logistical challenges or when immediate access to analytical equipment is not possible. Additionally, WCBs may be used alongside more complex analytical techniques to further confirm the results obtained.

WCBs hold great promise as accessible and versatile tools, and the abundance of academic literature addressing the subject attests to their utility and potential. They are, however, not without their shortcomings as selectivity can be an issue. Colorimetric biosensors are veritable assets enabling relatively quick and resource-efficient assessments of contamination in water and soil alike and can provide robust qualitative as well as quantitative measurements. The synthesis of microbial pigments is metabolically burdensome to microorganisms, and the genetic circuitry enabling these syntheses can be complex, which renders the development of colorimetric biosensors a less than straightforward endeavor. Nevertheless, future developments in biotechnology and a growing roster of known regulatory and pigment production pathways can enable further refinements of the protocols summarized in this review and the development of more advanced systems with greater precision, specificity, and range of detection. Moreover, an increased adoption of design of experiment or DoE methodologies could contribute quite positively to biosensor design, and the development of novel immobilization techniques can further improve their relevant attributes [110].

Author Contributions: G.N.: investigation, writing—original draft, writing—review and editing, formal analysis. M.K. and N.L.: conceptualization, supervision, writing—review and editing, formal analysis. L.E.C. and R.G.M.: formal analysis, writing—review and editing. All authors have read and agreed to the published version of the manuscript.

Funding: This work was funded by Campus France, the University of Saint-Joseph in Beirut's Research Council (Lebanon), and the "Université de Technologie de Compiègne, France".

Institutional Review Board Statement: Not applicable.

Informed Consent Statement: Not applicable.

Data Availability Statement: Data are contained within the article.

Conflicts of Interest: The authors declare no conflicts of interest.

References

1. Bousse, L. Whole Cell Biosensors. *Sens. Actuators B Chem.* **1996**, *34*, 270–275. [\[CrossRef\]](#)
2. Bhalla, N.; Jolly, P.; Formisano, N.; Estrela, P. Introduction to Biosensors. *Essays Biochem.* **2016**, *60*, 1–8. [\[CrossRef\]](#) [\[PubMed\]](#)
3. Wang, B.; Barahona, M.; Buck, M. A Modular Cell-Based Biosensor Using Engineered Genetic Logic Circuits to Detect and Integrate Multiple Environmental Signals. *Biosens. Bioelectron.* **2013**, *40*, 368–376. [\[CrossRef\]](#)
4. Wen, K.Y.; Rutter, J.W.; Barnes, C.P.; Dekker, L. Fundamental Building Blocks of Whole-Cell Biosensor Design. *Handb. Cell Biosens.* **2020**, 1–23. [\[CrossRef\]](#)
5. Khalil, A.S.; Collins, J.J. Synthetic Biology: Applications Come of Age. *Nat. Rev. Genet.* **2010**, *11*, 367–379. [\[CrossRef\]](#) [\[PubMed\]](#)
6. Hossain, G.S.; Saini, M.; Miyake, R.; Ling, H.; Chang, M.W. Genetic Biosensor Design for Natural Product Biosynthesis in Microorganisms. *Trends Biotechnol.* **2020**, *38*, 797–810. [\[CrossRef\]](#) [\[PubMed\]](#)
7. Serganov, A.; Nudler, E. A Decade of Riboswitches. *Cell* **2013**, *152*, 17–24. [\[CrossRef\]](#) [\[PubMed\]](#)
8. Wang, B.; Barahona, M.; Buck, M. Amplification of Small Molecule-Inducible Gene Expression via Tuning of Intracellular Receptor Densities. *Nucleic Acids Res.* **2015**, *43*, 1955–1964. [\[CrossRef\]](#)
9. Hui, C.Y.; Guo, Y.; Gao, C.X.; Li, H.; Lin, Y.R.; Yun, J.P.; Chen, Y.T.; Yi, J. A Tailored Indigoidine-Based Whole-Cell Biosensor for Detecting Toxic Cadmium in Environmental Water Samples. *Environ. Technol. Innov.* **2022**, *27*, 102511. [\[CrossRef\]](#)
10. Joe, M.H.; Lee, K.H.; Lim, S.Y.; Im, S.H.; Song, H.P.; Lee, I.S.; Kim, D.H. Pigment-Based Whole-Cell Biosensor System for Cadmium Detection Using Genetically Engineered *Deinococcus Radiodurans*. *Bioprocess Biosyst. Eng.* **2012**, *35*, 265–272. [\[CrossRef\]](#)
11. Liu, J.; Xu, J.Z.; Rao, Z.M.; Zhang, W.G. An Enzymatic Colorimetric Whole-Cell Biosensor for High-Throughput Identification of Lysine Overproducers. *Biosens. Bioelectron.* **2022**, *216*, 114681. [\[CrossRef\]](#) [\[PubMed\]](#)
12. Watstein, D.M.; Styczynski, M.P. Development of a Pigment-Based Whole-Cell Zinc Biosensor for Human Serum. *ACS Synth. Biol.* **2018**, *7*, 267–275. [\[CrossRef\]](#)
13. Chong, H.; Ching, C.B. Development of Colorimetric-Based Whole-Cell Biosensor for Organophosphorus Compounds by Engineering Transcription Regulator DmpR. *ACS Synth. Biol.* **2016**, *5*, 1290–1298. [\[CrossRef\]](#)
14. Carpenter, D.O. Polychlorinated Biphenyls (PCBs): Routes of Exposure and Effects on Human Health. *Rev. Environ. Health* **2006**, *21*, 1–23. [\[CrossRef\]](#)
15. Přibyl, J.; Hepel, M.; Skládal, P. Piezoelectric Immunosensors for Polychlorinated Biphenyls Operating in Aqueous and Organic Phases. *Sens. Actuators B Chem.* **2006**, *113*, 900–910. [\[CrossRef\]](#)
16. Shimomura, M.; Nomura, Y.; Zhang, W.; Sakino, M.; Lee, K.H.; Ikebukuro, K.; Karube, I. Simple and Rapid Detection Method Using Surface Plasmon Resonance for Dioxins, Polychlorinated Biphenyls and Atrazine. *Anal. Chim. Acta* **2001**, *434*, 223–230. [\[CrossRef\]](#)
17. Gavlasova, P.; Kuncova, G.; Kochankova, L.; Mackova, M. Whole Cell Biosensor for Polychlorinated Biphenyl Analysis Based on Optical Detection. *Int. Biodeterior. Biodegrad.* **2008**, *62*, 304–312. [\[CrossRef\]](#)
18. Dercová, K.; Baláž, Š.; Vrana, B.; Tandler, R. Aerobic Biodegradation of Polychlorinated Biphenyls (PCBs). In *The Utilization of Bioremediation to Reduce Soil Contamination: Problems and Solutions*; Springer: Dordrecht, The Netherlands, 2003; pp. 95–113. [\[CrossRef\]](#)
19. Nováková, H.; Vošahlíková, M.; Pazlarová, J.; Macková, M.; Burkhard, J.; Demnerová, K. PCB Metabolism by *Pseudomonas* Sp. P2. *Int. Biodeterior. Biodegrad.* **2002**, *50*, 47–54. [\[CrossRef\]](#)
20. Kuncova, G.; Berkova, D.; Burkhard, J.; Demnerova, K.; Pazlarova, J.; Triska, J.; Vrchotova, N. Optical Detection of Polychlorinated Biphenyls. In *Environmental Monitoring and Remediation Technologies II*; Vo-Dinh, T., Spellicy, R.L., Eds.; SPIE: Bellingham, WA, USA, 1999; Volume 3853, pp. 72–80.
21. Mulchandani, A.; Rajesh. Microbial Biosensors for Organophosphate Pesticides. *Appl. Biochem. Biotechnol.* **2011**, *165*, 687–699. [\[CrossRef\]](#)
22. Kumar, J.; Jha, S.K.; D'Souza, S.F. Optical Microbial Biosensor for Detection of Methyl Parathion Pesticide Using *Flavobacterium* Sp. Whole Cells Adsorbed on Glass Fiber Filters as Disposable Biocomponent. *Biosens. Bioelectron.* **2006**, *21*, 2100–2105. [\[CrossRef\]](#)

23. Wise, A.A.; Kuske, C.R. Generation of Novel Bacterial Regulatory Proteins That Detect Priority Pollutant Phenols. *Appl. Environ. Microbiol.* **2000**, *66*, 163–169. [\[CrossRef\]](#)
24. Pavel, H.; Forsman, M.; Shingler, V. An Aromatic Effector Specificity Mutant of the Transcriptional Regulator DmpR Overcomes the Growth Constraints of *Pseudomonas* Sp. Strain CF600 on Para-Substituted Methylphenols. *J. Bacteriol.* **1994**, *176*, 7550–7557. [\[CrossRef\]](#)
25. Campos, V.L.; Zaror, C.A.; Mondaca, M.A. Detection of Chlorinated Phenols in Kraft Pulp Bleaching Effluents Using DmpR Mutant Strains. *Bull. Environ. Contam. Toxicol.* **2004**, *73*, 666–673. [\[CrossRef\]](#) [\[PubMed\]](#)
26. Eger, A.; Koele, N.; Caspari, T.; Poggio, M.; Kumar, K.; Burge, O.R. Quantifying the Importance of Soil-Forming Factors Using Multivariate Soil Data at Landscape Scale. *J. Geophys. Res. Earth Surf.* **2021**, *126*, 1–19. [\[CrossRef\]](#)
27. Baumhardt, R.L.; Stewart, B.A.; Sainju, U.M. North American Soil Degradation: Processes, Practices, and Mitigating Strategies. *Sustainability* **2015**, *7*, 2936–2960. [\[CrossRef\]](#)
28. Turdean, G.L. Design and Development of Biosensors for the Detection of Heavy Metal Toxicity. *Int. J. Electrochem.* **2011**, *2011*, 1–15. [\[CrossRef\]](#)
29. Fei, X.; Lou, Z.; Xiao, R.; Ren, Z.; Lv, X. Contamination Assessment and Source Apportionment of Heavy Metals in Agricultural Soil through the Synthesis of PMF and GeogDetector Models. *Sci. Total Environ.* **2020**, *747*, 141293. [\[CrossRef\]](#)
30. Nies, D.H. Heavy Metal-Resistant Bacteria as Extremophiles: Molecular Physiology and Biotechnological Use of *Ralstonia* Sp. CH34. *Extremophiles* **2000**, *4*, 77–82. [\[CrossRef\]](#)
31. Knight, S.A.B.; Tamai, K.T.; Kosman, D.J.; Thiele, D.J. Identification and Analysis of a *Saccharomyces Cerevisiae* Copper Homeostasis Gene Encoding a Homeodomain Protein. *Mol. Cell. Biol.* **1994**, *14*, 7792–7804. [\[CrossRef\]](#)
32. Vopálenská, I.; Váchová, L.; Palková, Z. New Biosensor for Detection of Copper Ions in Water Based on Immobilized Genetically Modified Yeast Cells. *Biosens. Bioelectron.* **2015**, *72*, 160–167. [\[CrossRef\]](#)
33. Henikoff, S. The *Saccharomyces Cerevisiae* ADE5,7 Protein Is Homologous to Overlapping *Drosophila Melanogaster* Gatt Polypeptides. *J. Mol. Biol.* **1986**, *190*, 519–528. [\[CrossRef\]](#)
34. Shetty, R.S.; Deo, S.K.; Liu, Y.; Daunert, S. Fluorescence-Based Sensing System for Copper Using Genetically Engineered Living Yeast Cells. *Biotechnol. Bioeng.* **2004**, *88*, 664–670. [\[CrossRef\]](#)
35. Chen, P.H.; Lin, C.; Guo, K.H.; Yeh, Y.C. Development of a Pigment-Based Whole-Cell Biosensor for the Analysis of Environmental Copper. *RSC Adv.* **2017**, *7*, 29302–29305. [\[CrossRef\]](#)
36. Kumar, A.; Subrahmanyam, G.; Mondal, R.; Cabral-Pinto, M.M.S.; Shabnam, A.A.; Jigyasu, D.K.; Malyan, S.K.; Fagodiya, R.K.; Khan, S.A.; Yu, Z.G. Bio-Remediation Approaches for Alleviation of Cadmium Contamination in Natural Resources. *Chemosphere* **2021**, *268*, 128855. [\[CrossRef\]](#)
37. Hui, C.Y.; Hu, S.Y.; Li, L.M.; Yun, J.P.; Zhang, Y.F.; Yi, J.; Zhang, N.X.; Guo, Y. Metabolic Engineering of the Carotenoid Biosynthetic Pathway toward a Specific and Sensitive Inorganic Mercury Biosensor. *RSC Adv.* **2022**, *12*, 36142–36148. [\[CrossRef\]](#)
38. Meima, R.; Lindstrom, M.E. Characterization of the Minimal Replicon of a Cryptic *Deinococcus Radiodurans* SARK Plasmid and Development of Versatile *Escherichia Coli*-D. *Radiodurans* Shuttle Vectors. *Appl. Environ. Microbiol.* **2000**, *66*, 3856–3867. [\[CrossRef\]](#) [\[PubMed\]](#)
39. Joe, M.H.; Jung, S.W.; Im, S.H.; Lim, S.Y.; Song, H.P.; Kwon, O.; Kim, D.H. Genome-Wide Response of *Deinococcus Radiodurans* on Cadmium Toxicity. *J. Microbiol. Biotechnol.* **2011**, *21*, 438–447. [\[CrossRef\]](#) [\[PubMed\]](#)
40. Hui, C.Y.; Guo, Y.; Li, H.; Gao, C.X.; Yi, J. Detection of Environmental Pollutant Cadmium in Water Using a Visual Bacterial Biosensor. *Sci. Rep.* **2022**, *12*, 1–11. [\[CrossRef\]](#) [\[PubMed\]](#)
41. Lee, S.W.; Glickmann, E.; Cooksey, D.A. Chromosomal Locus for Cadmium Resistance in *Pseudomonas Putida* Consisting of a Cadmium-Transporting ATPase and a MerR Family Response Regulator. *Appl. Environ. Microbiol.* **2001**, *67*, 1437–1444. [\[CrossRef\]](#) [\[PubMed\]](#)
42. August, P.R.; Grossman, T.H.; Minor, C.; Draper, M.P.; MacNeil, I.A.; Pemberton, J.M.; Call, K.M.; Holt, D.; Osbourne, S. Sequence Analysis and Functional Characterization of the Violacein Biosynthetic Pathway from *Chromobacterium Violaceum*. *J. Mol. Microbiol. Biotechnol.* **2000**, *2*, 513–519. [\[PubMed\]](#)
43. Hui, C.Y.; Guo, Y.; Liu, L.; Zhang, N.X.; Gao, C.X.; Yang, X.Q.; Yi, J. Genetic Control of Violacein Biosynthesis to Enable a Pigment-Based Whole-Cell Lead Biosensor. *RSC Adv.* **2020**, *10*, 28106–28113. [\[CrossRef\]](#)
44. Shahid, M.; Dumat, C.; Khalid, S.; Niazi, N.K.; Antunes, P.M.C. Cadmium Bioavailability, Uptake, Toxicity and Detoxification in Soil-Plant System. In *How to Recruit Voluntary Donors in the Third World?* Springer: Cham, Switzerland, 2016; Volume 238, pp. 73–137.
45. Brocklehurst, K.R.; Megit, S.J.; Morby, A.P. Characterisation of CadR from *Pseudomonas Aeruginosa*: A Cd(II)-Responsive MerR Homologue. *Biochem. Biophys. Res. Commun.* **2003**, *308*, 234–239. [\[CrossRef\]](#)
46. Liu, X.; Hu, Q.; Yang, J.; Huang, S.; Wei, T.; Chen, W.; He, Y.; Wang, D.; Liu, Z.; Wang, K.; et al. Selective Cadmium Regulation Mediated by a Cooperative Binding Mechanism in CadR. *Proc. Natl. Acad. Sci. USA* **2019**, *116*, 20398–20403. [\[CrossRef\]](#)
47. Hui, C.Y.; Guo, Y.; Li, L.M.; Liu, L.; Chen, Y.T.; Yi, J.; Zhang, N.X. Indigoidine Biosynthesis Triggered by the Heavy Metal-Responsive Transcription Regulator: A Visual Whole-Cell Biosensor. *Appl. Microbiol. Biotechnol.* **2021**, *105*, 6087–6102. [\[CrossRef\]](#)
48. Hui, C.Y.; Guo, Y.; Wu, J.; Liu, L.; Yang, X.Q.; Guo, X.; Xie, Y.; Yi, J. Detection of Bioavailable Cadmium by Double-Color Fluorescence Based on a Dual-Sensing Bioreporter System. *Front. Microbiol.* **2021**, *12*, 1–15. [\[CrossRef\]](#)

49. Tian, H.; Jiao, L.; Dong, D. Rapid Determination of Trace Cadmium in Drinking Water Using Laser-Induced Breakdown Spectroscopy Coupled with Chelating Resin Enrichment. *Sci. Rep.* **2019**, *9*, 1–8. [\[CrossRef\]](#) [\[PubMed\]](#)
50. Davis, A.; Wu, P.; Zhang, X.; Hou, X.; Jones, B. Determination of Cadmium in Biological Samples. *Appl. Spectrosc. Rev.* **2006**, *41*, 35–75. [\[CrossRef\]](#)
51. Büyükpınar, Ç.; Bodur, S.; Yazıcı, E.; Tekin, Z.; San, N.; Tarık Komesli, O.; Bakırdere, S. An Accurate Analytical Method for the Determination of Cadmium: Ultraviolet Based Photochemical Vapor Generation-Slotted Quartz Tube Based Atom Trap-Flame Atomic Absorption Spectrophotometry. *Meas. J. Int. Meas. Confed.* **2021**, *176*, 109192. [\[CrossRef\]](#)
52. Wei, W.; Liu, X.; Sun, P.; Wang, X.; Zhu, H.; Hong, M.; Mao, Z.W.; Zhao, J. Simple Whole-Cell Biodetection and Bioremediation of Heavy Metals Based on an Engineered Lead-Specific Operon. *Environ. Sci. Technol.* **2014**, *48*, 3363–3371. [\[CrossRef\]](#) [\[PubMed\]](#)
53. Shetty, R.S.; Deo, S.K.; Shah, P.; Sun, Y.; Rosen, B.P.; Daunert, S. Luminescence-Based Whole-Cell-Sensing Systems for Cadmium and Lead Using Genetically Engineered Bacteria. *Anal. Bioanal. Chem.* **2003**, *376*, 11–17. [\[CrossRef\]](#) [\[PubMed\]](#)
54. Borremans, B.; Hobman, J.L.; Provoost, A.; Brown, N.L.; Van Der Lelie, D. Cloning and Functional Analysis of the Pbr Lead Resistance Determinant of *Ralstonia Metallidurans* CH34. *J. Bacteriol.* **2001**, *183*, 5651–5658. [\[CrossRef\]](#) [\[PubMed\]](#)
55. Hui, C.; Ma, B.; Wang, Y.; Yang, X.; Cai, J. Designed Bacteria Based on Natural Pbr Operons for Detecting and Detoxifying Environmental Lead: A Mini-Review. *Ecotoxicol. Environ. Saf.* **2023**, *267*, 115662. [\[CrossRef\]](#) [\[PubMed\]](#)
56. Bereza-Malcolm, L.; Aracic, S.; Franks, A.E. Development and Application of a Synthetically-Derived Lead Biosensor Construct for Use in Gram-Negative Bacteria. *Sensors* **2016**, *16*, 2174. [\[CrossRef\]](#) [\[PubMed\]](#)
57. Nourmohammadi, E.; Hosseinkhani, S.; Nedaeinia, R.; Khoshdel-Sarkarizi, H.; Nedaeinia, M.; Ranjbar, M.; Ebrahimi, N.; Farjami, Z.; Nourmohammadi, M.; Mahmoudi, A.; et al. Construction of a Sensitive and Specific Lead Biosensor Using a Genetically Engineered Bacterial System with a Luciferase Gene Reporter Controlled by Pbr and CadA Promoters. *Biomed. Eng. Online* **2020**, *19*, 1–13. [\[CrossRef\]](#) [\[PubMed\]](#)
58. Jia, X.; Zhao, T.; Liu, Y.; Bu, R.; Wu, K. Gene Circuit Engineering to Improve the Performance of a Whole-Cell Lead Biosensor. *FEMS Microbiol. Lett.* **2018**, *365*, 1–8. [\[CrossRef\]](#) [\[PubMed\]](#)
59. Guo, Y.; Hui, C.Y.; Liu, L.; Zheng, H.Q.; Wu, H.M. Improved Monitoring of Low-Level Transcription in *Escherichia Coliby* a β -Galactosidase α -Complementation System. *Front. Microbiol.* **2019**, *10*, 1–12. [\[CrossRef\]](#)
60. Hui, C.Y.; Guo, Y.; Zhu, D.L.; Li, L.M.; Yi, J.; Zhang, N.X. Metabolic Engineering of the Violacein Biosynthetic Pathway toward a Low-Cost, Minimal-Equipment Lead Biosensor. *Biosens. Bioelectron.* **2022**, *214*, 114531. [\[CrossRef\]](#)
61. Zhao, E.M.; Suek, N.; Wilson, M.Z.; Dine, E.; Pannucci, N.L.; Gitai, Z.; Avalos, J.L.; Toettcher, J.E. Light-Based Control of Metabolic Flux through Assembly of Synthetic Organelles. *Nat. Chem. Biol.* **2019**, *15*, 589–597. [\[CrossRef\]](#)
62. Guo, Y.; Huang, Z.L.; Zhu, D.L.; Hu, S.Y.; Li, H.; Hui, C.Y. Anthocyanin Biosynthetic Pathway Switched by Metalloregulator PbrR to Enable a Biosensor for the Detection of Lead Toxicity. *Front. Microbiol.* **2022**, *13*, 1–10. [\[CrossRef\]](#)
63. Miyazawa, T.; Nakagawa, K.; Kudo, M.; Muraishi, K.; Someya, K. Direct Intestinal Absorption of Red Fruit Anthocyanins, Cyanidin-3- Glucoside and Cyanidin-3,5-Diglucoside, into Rats and Humans. *J. Agric. Food Chem.* **1999**, *47*, 1083–1091. [\[CrossRef\]](#) [\[PubMed\]](#)
64. Olivas-Aguirre, F.J.; Rodrigo-García, J.; Martínez-Ruiz, N.D.R.; Cárdenas-Robles, A.I.; Mendoza-Díaz, S.O.; Álvarez-Parrilla, E.; González-Aguilar, G.A.; De La Rosa, L.A.; Ramos-Jiménez, A.; Wall-Medrano, A. Cyanidin-3-O-Glucoside: Physical-Chemistry, Foodomics and Health Effects. *Molecules* **2016**, *21*, 1264. [\[CrossRef\]](#) [\[PubMed\]](#)
65. Masten, S.J.; Davies, S.H.; McElmurry, S.P. Flint Water Crisis: What Happened and Why? *J. Am. Water Works Assoc.* **2016**, *108*, 22–34. [\[CrossRef\]](#) [\[PubMed\]](#)
66. Helmann, J.D.; Ballard, B.T.; Walsh, C.T. The MerR Metalloregulatory Protein Binds Mercuric Ion as a Tricoordinate, Metal-Bridged Dimer. *Science* **1990**, *247*, 946–948. [\[CrossRef\]](#) [\[PubMed\]](#)
67. Zhang, N.X.; Guo, Y.; Li, H.; Yang, X.Q.; Gao, C.X.; Hui, C.Y. Versatile Artificial Mer Operons in *Escherichia Coli* towards Whole Cell Biosensing and Adsorption of Mercury. *PLoS ONE* **2021**, *16*, 1–14. [\[CrossRef\]](#) [\[PubMed\]](#)
68. Guo, Y.; Hui, C.Y.; Liu, L.; Chen, M.P.; Huang, H.Y. Development of a Bioavailable Hg(II) Sensing System Based on MerR-Regulated Visual Pigment Biosynthesis. *Sci. Rep.* **2021**, *11*, 1–13. [\[CrossRef\]](#)
69. Huang, L.; Huang, Y.; Lou, Y.; Qian, H.; Xu, D.; Ma, L.; Jiang, C.; Zhang, D. Pyocyanin-Modifying Genes PhzM and PhzS Regulated the Extracellular Electron Transfer in Microbiologically-Influenced Corrosion of X80 Carbon Steel by *Pseudomonas Aeruginosa*. *Corros. Sci.* **2020**, *164*, 108355. [\[CrossRef\]](#)
70. Wang, D.; Zheng, Y.; Fan, X.; Xu, L.; Pang, T.; Liu, T.; Liang, L.; Huang, S.; Xiao, Q. Visual Detection of Hg²⁺ by Manipulation of Pyocyanin Biosynthesis through the Hg²⁺-Dependent Transcriptional Activator MerR in Microbial Cells. *J. Biosci. Bioeng.* **2020**, *129*, 223–228. [\[CrossRef\]](#) [\[PubMed\]](#)
71. Ketelboeter, L.M.; Bardy, S.L. Methods to Inhibit Bacterial Pyomelanin Production and Determine the Corresponding Increase in Sensitivity to Oxidative Stress. *J. Vis. Exp.* **2015**, *2015*, 1–9. [\[CrossRef\]](#)
72. De Mora, K.; Joshi, N.; Balint, B.L.; Ward, F.B.; Elfick, A.; French, C.E. A PH-Based Biosensor for Detection of Arsenic in Drinking Water. *Anal. Bioanal. Chem.* **2011**, *400*, 1031–1039. [\[CrossRef\]](#)
73. Wu, J.; Rosen, B.P. The ArsR Protein Is a Trans-acting Regulatory Protein. *Mol. Microbiol.* **1991**, *5*, 1331–1336. [\[CrossRef\]](#)
74. Fujimoto, H.; Wakabayashi, M.; Yamashiro, H.; Maeda, I.; Isoda, K.; Kondoh, M.; Kawase, M.; Miyasaka, H.; Yagi, K. Whole-Cell Arsenite Biosensor Using Photosynthetic Bacterium *Rhodovulum Sulfidophilum*: *Rhodovulum Sulfidophilum* as an Arsenite Biosensor. *Appl. Microbiol. Biotechnol.* **2006**, *73*, 332–338. [\[CrossRef\]](#)

75. Yoshida, K.; Inoue, K.; Takahashi, Y.; Ueda, S.; Isoda, K.; Yagi, K.; Maeda, I. Novel Carotenoid-Based Biosensor for Simple Visual Detection of Arsenite: Characterization and Preliminary Evaluation for Environmental Application. *Appl. Environ. Microbiol.* **2008**, *74*, 6730–6738. [\[CrossRef\]](#)
76. Yoshida, K.; Yoshioka, D.; Inoue, K.; Takaichi, S.; Maeda, I. Evaluation of Colors in Green Mutants Isolated from Purple Bacteria as a Host for Colorimetric Whole-Cell Biosensors. *Appl. Microbiol. Biotechnol.* **2007**, *76*, 1043–1050. [\[CrossRef\]](#) [\[PubMed\]](#)
77. Zaynab, M.; Al-Yahyai, R.; Ameen, A.; Sharif, Y.; Ali, L.; Fatima, M.; Khan, K.A.; Li, S. Health and Environmental Effects of Heavy Metals. *J. King Saud Univ.-Sci.* **2022**, *34*, 101653. [\[CrossRef\]](#)
78. Ali, H.; Khan, E. Trophic Transfer, Bioaccumulation, and Biomagnification of Non-Essential Hazardous Heavy Metals and Metalloids in Food Chains/Webs—Concepts and Implications for Wildlife and Human Health. *Hum. Ecol. Risk Assess.* **2019**, *25*, 1353–1376. [\[CrossRef\]](#)
79. Li, C.; Zhou, K.; Qin, W.; Tian, C.; Qi, M.; Yan, X.; Han, W. A Review on Heavy Metals Contamination in Soil: Effects, Sources, and Remediation Techniques. *Soil Sediment Contam.* **2019**, *28*, 380–394. [\[CrossRef\]](#)
80. Gupta, A.; Sharma, V.; Sharma, K.; Kumar, V.; Choudhary, S.; Mankotia, P.; Kumar, B.; Mishra, H.; Moulick, A.; Ekielski, A.; et al. A Review of Adsorbents for Heavy Metal Decontamination: Growing Approach to Wastewater Treatment. *Materials* **2021**, *14*, 4702. [\[CrossRef\]](#) [\[PubMed\]](#)
81. Kumar, V.; Rout, C.; Singh, J.; Saharan, Y.; Goyat, R.; Umar, A.; Akbar, S.; Baskoutas, S. A Review on the Clean-up Technologies for Heavy Metal Ions Contaminated Soil Samples. *Heliyon* **2023**, *9*, e15472. [\[CrossRef\]](#) [\[PubMed\]](#)
82. Félix, F.K. do C.; Letti, L.A.J.; Vinícius de Melo Pereira, G.; Bonfim, P.G.B.; Soccol, V.T.; Soccol, C.R. L-Lysine Production Improvement: A Review of the State of the Art and Patent Landscape Focusing on Strain Development and Fermentation Technologies. *Crit. Rev. Biotechnol.* **2019**, *39*, 1031–1055. [\[CrossRef\]](#) [\[PubMed\]](#)
83. Cheng, J.; Chen, P.; Song, A.; Wang, D.; Wang, Q. Expanding Lysine Industry: Industrial Biomanufacturing of Lysine and Its Derivatives. *J. Ind. Microbiol. Biotechnol.* **2018**, *45*, 719–734. [\[CrossRef\]](#)
84. Ikeda, M. Lysine Fermentation: History and Genome Breeding. In *Advances in Biochemical Engineering/Biotechnology*; Springer: Tokyo, Japan, 2016; Volume 123, pp. 73–102.
85. Bellman, A.; Vrljić, M.; Pátek, M.; Sahm, H.; Krämer, R.; Eggeling, L. Expression Control and Specificity of the Basic Amino Acid Exporter LysE of *Corynebacterium Glutamicum*. *Microbiology* **2001**, *147*, 1765–1774. [\[CrossRef\]](#)
86. Henke, N.A.; Wendisch, V.F. Improved Astaxanthin Production with *Corynebacterium Glutamicum* by Application of a Membrane Fusion Protein. *Mar. Drugs* **2019**, *17*, 621. [\[CrossRef\]](#)
87. Kumari, A.; Pasini, P.; Daunert, S. Detection of Bacterial Quorum Sensing N-Acyl Homoserine Lactones in Clinical Samples. *Anal. Bioanal. Chem.* **2008**, *391*, 1619–1627. [\[CrossRef\]](#)
88. Yeon, K.M.; Cheong, W.S.; Oh, H.S.; Lee, W.N.; Hwang, B.K.; Lee, C.H.; Beyenal, H.; Lewandowski, Z. Quorum Sensing: A New Biofouling Control Paradigm in a Membrane Bioreactor for Advanced Wastewater Treatment. *Environ. Sci. Technol.* **2009**, *43*, 380–385. [\[CrossRef\]](#)
89. Valle, A.; Bailey, M.J.; Whiteley, A.S.; Manefield, M. N-Acyl-L-Homoserine Lactones (AHLs) Affect Microbial Community Composition and Function in Activated Sludge. *Environ. Microbiol.* **2004**, *6*, 424–433. [\[CrossRef\]](#)
90. Song, S.; Jia, Z.; Xu, J.; Zhang, Z.; Bian, Z. N-Butyryl-Homoserine Lactone, a Bacterial Quorum-Sensing Signaling Molecule, Induces Intracellular Calcium Elevation in Arabidopsis Root Cells. *Biochem. Biophys. Res. Commun.* **2011**, *414*, 355–360. [\[CrossRef\]](#) [\[PubMed\]](#)
91. Yong, Y.C.; Zhong, J.J. A Genetically Engineered Whole-Cell Pigment-Based Bacterial Biosensing System for Quantification of N-Butyryl Homoserine Lactone Quorum Sensing Signal. *Biosens. Bioelectron.* **2009**, *25*, 41–47. [\[CrossRef\]](#) [\[PubMed\]](#)
92. Sun, G.X.; Zhou, W.Q.; Zhong, J.J. Organotin Decomposition by Pyochelin, Secreted by *Pseudomonas Aeruginosa* Even in an Iron-Sufficient Environment. *Appl. Environ. Microbiol.* **2006**, *72*, 6411–6413. [\[CrossRef\]](#) [\[PubMed\]](#)
93. Wu, Y.; Wang, C.W.; Wang, D.; Wei, N. A Whole-Cell Biosensor for Point-of-Care Detection of Waterborne Bacterial Pathogens. *ACS Synth. Biol.* **2021**, *10*, 333–344. [\[CrossRef\]](#) [\[PubMed\]](#)
94. D’Agata, E.M.C.; Dupont-Rouzeyrol, M.; Magal, P.; Olivier, D.; Ruan, S. The Impact of Different Antibiotic Regimens on the Emergence of Antimicrobial-Resistant Bacteria. *PLoS ONE* **2008**, *3*, 4–12. [\[CrossRef\]](#) [\[PubMed\]](#)
95. Dou, Y.; Song, F.; Guo, F.; Zhou, Z.; Zhu, C.; Xiang, J.; Huan, J. *Acinetobacter Baumannii* Quorum-Sensing Signalling Molecule Induces the Expression of Drug-Resistance Genes. *Mol. Med. Rep.* **2017**, *15*, 4061–4068. [\[CrossRef\]](#)
96. Saipriya, K.; Swathi, C.H.; Ratnakar, K.S.; Sritharan, V. Quorum-Sensing System in *Acinetobacter Baumannii*: A Potential Target for New Drug Development. *J. Appl. Microbiol.* **2020**, *128*, 15–27. [\[CrossRef\]](#)
97. Haque, S.; Yadav, D.K.; Bisht, S.C.; Yadav, N.; Singh, V.; Dubey, K.K.; Jawed, A.; Wahid, M.; Dar, S.A. Quorum Sensing Pathways in Gram-Positive and -Negative Bacteria: Potential of Their Interruption in Abating Drug Resistance. *J. Chemother.* **2019**, *31*, 161–187. [\[CrossRef\]](#)
98. Zhao, X.; Yu, Z.; Ding, T. Quorum-Sensing Regulation of Antimicrobial Resistance in Bacteria. *Microorganisms* **2020**, *8*, 425. [\[CrossRef\]](#)
99. Stock, F.; Cirri, E.; Nuwanthi, S.G.L.I.; Stock, W.; Ueberschaar, N.; Mangelinckx, S.; Pohnert, G.; Vyverman, W. Sampling, Separation, and Quantification of N-Acyl Homoserine Lactones from Marine Intertidal Sediments. *Limnol. Oceanogr. Methods* **2021**, *19*, 145–157. [\[CrossRef\]](#)

100. Hoang, T.P.T.; Barthélemy, M.; Lami, R.; Stien, D.; Eparvier, V.; Touboul, D. Annotation and Quantification of N-Acyl Homoserine Lactones Implied in Bacterial Quorum Sensing by Supercritical-Fluid Chromatography Coupled with High-Resolution Mass Spectrometry. *Anal. Bioanal. Chem.* **2020**, *412*, 2261–2276. [[CrossRef](#)] [[PubMed](#)]
101. Rodrigues, A.M.S.; Lami, R.; Escoubeyrou, K.; Intertaglia, L.; Mazurek, C.; Doberva, M.; Pérez-Ferrer, P.; Stien, D. Straightforward N -Acyl Homoserine Lactone Discovery and Annotation by LC–MS/MS-Based Molecular Networking. *J. Proteome Res.* **2022**, *21*, 635–642. [[CrossRef](#)] [[PubMed](#)]
102. Stevens, G.A.; Beal, T.; Mbuya, M.N.N.; Luo, H.; Neufeld, L.M.; Addo, O.Y.; Adu-Afarwuah, S.; Alayón, S.; Bhutta, Z.; Brown, K.H.; et al. Micronutrient Deficiencies among Preschool-Aged Children and Women of Reproductive Age Worldwide: A Pooled Analysis of Individual-Level Data from Population-Representative Surveys. *Lancet Glob. Health* **2022**, *10*, e1590–e1599. [[CrossRef](#)]
103. Wessells, K.R.; Brown, K.H. Estimating the Global Prevalence of Zinc Deficiency: Results Based on Zinc Availability in National Food Supplies and the Prevalence of Stunting. *PLoS ONE* **2012**, *7*. [[CrossRef](#)]
104. McNerney, M.P.; Michel, C.L.; Kishore, K.; Standeven, J.; Styczynski, M.P. Dynamic and Tunable Metabolite Control for Robust Minimal-Equipment Assessment of Serum Zinc. *Nat. Commun.* **2019**, *10*. [[CrossRef](#)] [[PubMed](#)]
105. Reyes, S.; Le, N.; Fuentes, M.D.; Upegui, J.; Dikici, E.; Broyles, D.; Quinto, E.; Daunert, S.; Deo, S.K. An Intact Cell Bioluminescence-Based Assay for the Simple and Rapid Diagnosis of Urinary Tract Infection. *Int. J. Mol. Sci.* **2020**, *21*, 5015. [[CrossRef](#)] [[PubMed](#)]
106. Lubkowicz, D.; Ho, C.L.; Hwang, I.Y.; Yew, W.S.; Lee, Y.S.; Chang, M.W. Reprogramming Probiotic *Lactobacillus Reuteri* as a Biosensor for *Staphylococcus Aureus* Derived AIP-I Detection. *ACS Synth. Biol.* **2018**, *7*, 1229–1237. [[CrossRef](#)] [[PubMed](#)]
107. Raut, N.; Pasini, P.; Daunert, S. Deciphering Bacterial Universal Language by Detecting the Quorum Sensing Signal, Autoinducer-2, with a Whole-Cell Sensing System. *Anal. Chem.* **2013**, *85*, 9604–9609. [[CrossRef](#)] [[PubMed](#)]
108. Woo, S.G.; Moon, S.J.; Kim, S.K.; Kim, T.H.; Lim, H.S.; Yeon, G.H.; Sung, B.H.; Lee, C.H.; Lee, S.G.; Hwang, J.H.; et al. A Designed Whole-Cell Biosensor for Live Diagnosis of Gut Inflammation through Nitrate Sensing. *Biosens. Bioelectron.* **2020**, *168*, 112523. [[CrossRef](#)]
109. Moraskie, M.; Roshid, H.; Connor, G.O.; Dikici, E.; Zingg, J.; Deo, S.; Daunert, S. Microbial Whole-Cell Biosensors: Current Applications, Challenges, and Future Perspectives. *Biosens. Bioelectron.* **2022**, *191*, 113359. [[CrossRef](#)]
110. Berepiki, A.; Kent, R.; MacHado, L.F.M.; Dixon, N. Development of High-Performance Whole Cell Biosensors Aided by Statistical Modeling. *ACS Synth. Biol.* **2020**, *9*, 576–589. [[CrossRef](#)]

Disclaimer/Publisher’s Note: The statements, opinions and data contained in all publications are solely those of the individual author(s) and contributor(s) and not of MDPI and/or the editor(s). MDPI and/or the editor(s) disclaim responsibility for any injury to people or property resulting from any ideas, methods, instructions or products referred to in the content.